國 立 交 通 大 學

電信工程研究所

碩 士 論 文

異質性無線網路之基地台間干擾控制技術

Inter-Cell Interference Control for Heterogeneous Wireless Networks in 3GPP LTE-Advanced Systems

研究生：周振孝

指導教授：王蒞君

中 華 民 國 一百零一年 六月

異質性無線網路之基地台間干擾控制技術

Inter-Cell Interference Control for Heterogeneous Wireless Networks in 3GPP LTE-Advanced Systems

研 究 生：周振孝　　Student：Chen-Hsiao Chou

指導教授：王蒞君　　Advisor：Li-Chun Wang

A Thesis

Submitted to Institute of Communications Engineering

College of Electrical and Computer Engineering

National Chiao Tung University

in partial Fulfillment of the Requirements

for the Degree of

Master of Science

In

Communication Engineering

June 2012

Hsinchu, Taiwan, Republic of China

中華民國 一百零一 年 六 月

異質性無線網路之基地台間干擾控制技術

學生：周振孝　　指導教授：王蒞君　教授

國立交通大學

電機學院電信工程研究所

摘要

在第三代合作夥伴計劃-長期演進技術的環境下，為了提供更高的資料傳輸速率以及提高頻譜使用效率，多基地台間合作式傳輸以及接收技術被視為可以有效地提供效益。在本篇論文中，在異質性無線網路之下，大基地台間以及大基地台範圍內布建的小基地台，都有光纖互相連結傳輸，我們提出在此系統下，可以結合各個大基地台間的合作，以及大基地台跟微小基地台間的合作傳輸技術。

由於要讓各個基地台間合作，在使用者手機端中需要去回饋通道資訊才能完成傳輸並且保持傳輸量，回饋到基地台的資訊會造成當接收完成後，通道情形已經改變，所以我們將這樣的延遲效應考慮進來，去比較延遲對系統效能的影響。在論文中，我們針對結合各種基地台間合作，提出一種可以有效改善頻譜效率的合作式傳輸技術；此外，再將提出的傳輸技術應用到不同的基地台架構下，也找出最適合的這項技術的架構。

Inter-Cell Interference Control for Heterogeneous Wireless Networks in 3GPP LTE-Advanced Systems

A THESIS Presented to

The Academic Faculty By

Chen-Hsiao Chou

In Partial Fulfillment

of the Requirements for the Degree of

Master in Communications Engineering

Institute of Communications Engineering

College of Electrical and Computer Engineering

National Chiao-Tung University

June, 2012

Abstract

Since there are more demands for high data rates, the 3^{rd} Generation Partnership Project (3GPP) has already published many researches and contributions about increasing the spectral efficiency. We have seen a lot of studies on coordinated multipoint transmission and reception techniques for the LTE-A systems. The main perspectives of these approaches aim at mitigating the inter-cell interference and also increasing the system performance. Recently, several coordinated multipoint (CoMP) transmission techniques have already been investigated. This thesis presents a joint cooperation design based on CoMP operations. Our design will combine cooperation between intra-site with remote radio head and inter-site with available backhaul. The gaol of this thesis is to evaluate the improvement by a joint design method and provide a better strategy when combining the cooperation of both sites. Since we try to extend CoMP region from intra-site to inter-site, we have to exchange more channel state information and data between devices. This will increase the feedback time to complete reception. We consider that the delay effect should be included and evaluated. In addition, we will discuss the effects upon the system performance which are caused by different cell architectures. Several CoMP transmission techniques are operated in heterogeneous network. We use different ones in inter-site cooperation to compare the system performance of spectrum efficiency. Compared with other transmission schemes, the proposed scheme is a feasible method to enhance spectral efficiency.

Acknowledgments

I would like to thank my parents and my older brother. They always give me endless supports. In every important time of my life, they always guide me and take care of me without asking anything in return. I especially thank Professor Li-Chun Wang who gave me many valuable suggestions in my research during these two years. I would not finish this work without his guidance and comments.

In addition, I am deeply grateful to my laboratory mates, Ssu-Han, Tsung-Ting, and junior laboratory mates at Mobile Communications and Cloud Computing Laboratory at the Institute of Communication Engineering in National Chiao-Tung University. They provide me much assistance and share much happiness with me.

Contents

List of Tables

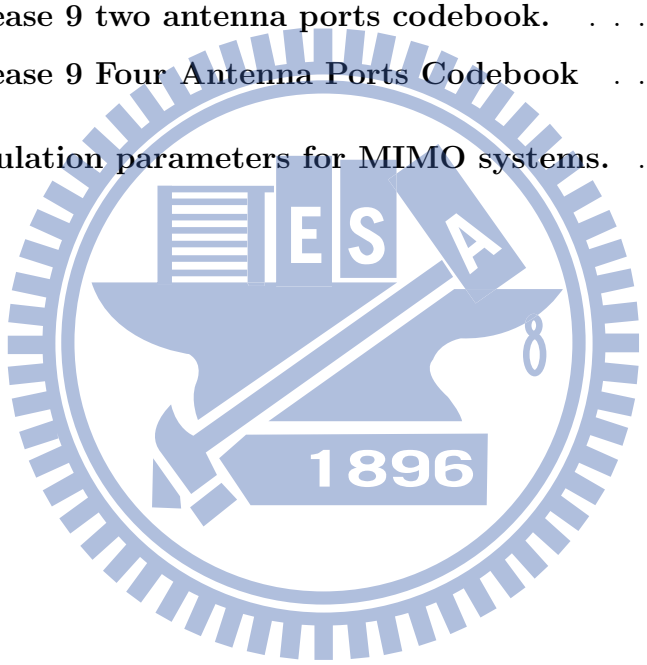

List of Figures

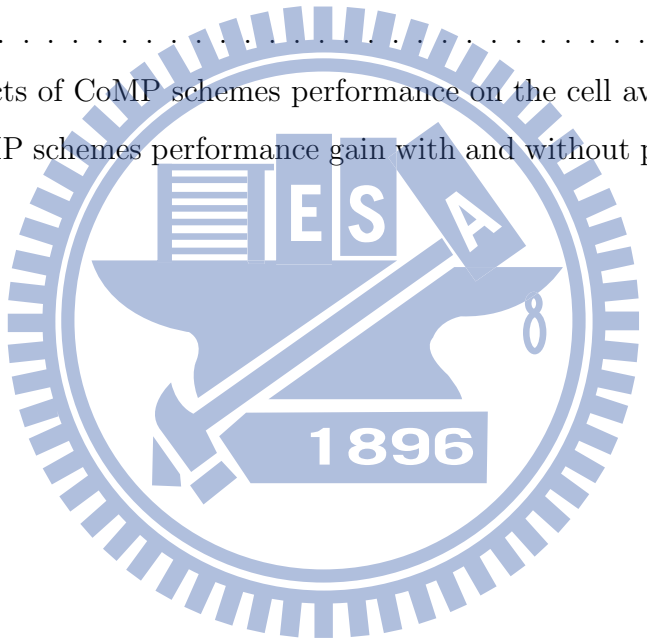


E S A
1896

CHAPTER 1

Introduction

In cellular systems, inter-cell interference is a serious issue, which degrades system performance. When a user is located at the serving cell edge, it will suffer from the inter-cell interference (ICI) caused by neighboring cell and has poor spectral efficiency. In the Long Term Evolution-Advanced (LTE-A) system, base stations are connected by a high speed backhaul (e.g. optical fiber) and form a cooperative set. All the base stations (BS) in this set can exchange information and share data with the backhaul. Thus, BSs can jointly perform MIMO processing to serve users at the same time by sharing channel state information and transmit data [1]. The network multiple-input multiple-output (MIMO), also referred to as coordinated multi-point transmission (CoMP) technique, becomes an important approach in both industry and academia, which aims to mitigate the ICI by coordinating transmission among different BSs [2]. For the target downlink peak spectral efficiency of 30 bps/Hz and uplink case of

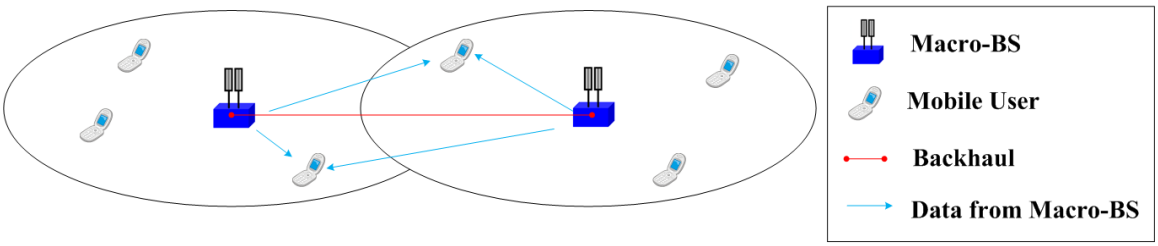

Figure 1.1: The CoMP MIMO systems.

15 bps/Hz, CoMP techniques are regarded as the effective and efficient methods in LTE-A. We categorize the CoMP schemes into the following different approaches, such as joint processing (JP), and coordinated scheduling and beamforming (CS/CB) transmission techniques [3].

1. **Joint Processing:** Data and channel state information (CSI) are available at a cooperation set which comprises multiple macro-cells for resource blocks.

   (a) *Joint Transmission:* A transmission scheme can provide simultaneous data transmission from multiple cells to single or multiple users in a resource block. All the data and CSI from multiple cells to multiple-user should be shared among the cooperation set.

   (b) *Dynamic point selection/muting:* Dynamic cell selection: Data transmission could be transmitted from the cell of a cooperation set. However, in each subframe, the transmitting/muting cell can be changed and may be different from dynamic selection/muting.

2. **Coordinated Scheduling/Beamforming:** The best example of conventional is the Good/Bad reporting algorithm, which is applied widely. This transmission scheme is accomplished by choosing a least interference precoding matrix indicator (PMI) from a recommended set, which can be sent from the cooperation cells. Every cell in this kind of cooperation needs to exchange and get the information about channel state and interference from serving cell to each user. The size of recommended set would be based on the tolerable interference level [4, 5].

According to [3], four CoMP scenarios are provided and discussed. BSs in each scenario can be connected and serve their users collaboratively by different cooperation techniques. We categorize the LTE-A environment in the following list.

1. *Scenario 1:* Homogeneous network with intra-site CoMP.

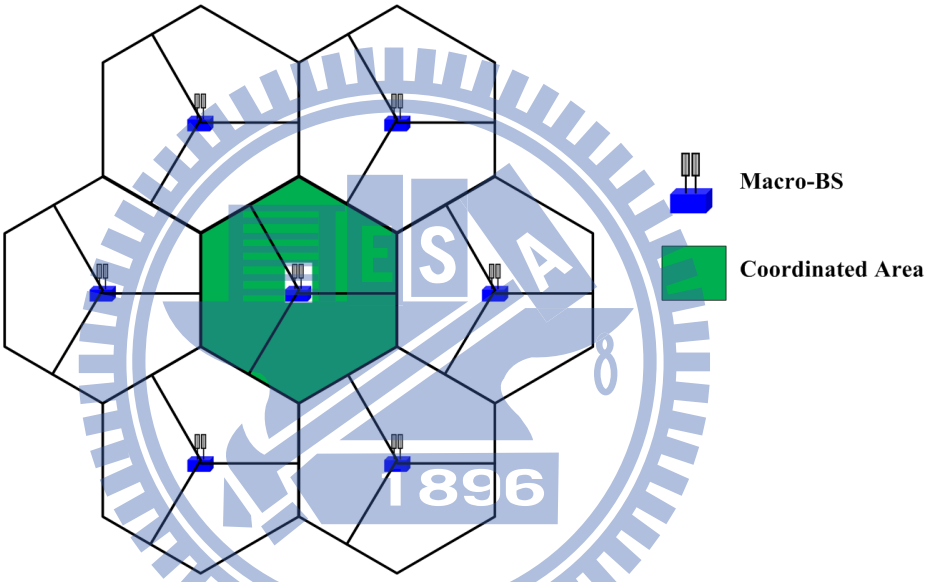

Figure 1.2: Scenario 1: Homogeneous network with intra-site CoMP.

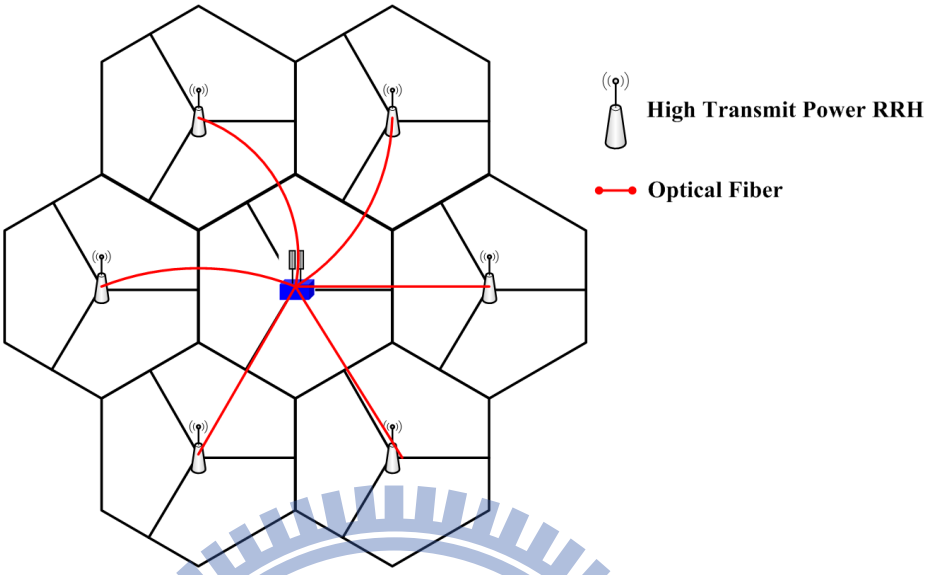

Figure 1.3: Scenario 2: Homogeneous network with high transmit power RRHs with intra CoMP.

2. *Scenario 2:* Homogeneous network with high transmit power remote radio heads (RRHs) with intra CoMP.

3. *Scenario 3:* Heterogeneous network with low transmit power RRH within the macro-cell coverage where transmission/reception points created by the RRHs have different cell IDs from the macro-cell.

4. *Scenario 4:* Heterogeneous network with low transmit power RRH within the macro-cell coverage where transmission/reception points created by the RRHs have the same cell IDs as the macro-cell.

Briefly, scenarios 1 and 2 are homogeneous network, and scenarios 3 and 4 are heterogeneous network (HetNet) with RRH within macro-cell coverage.

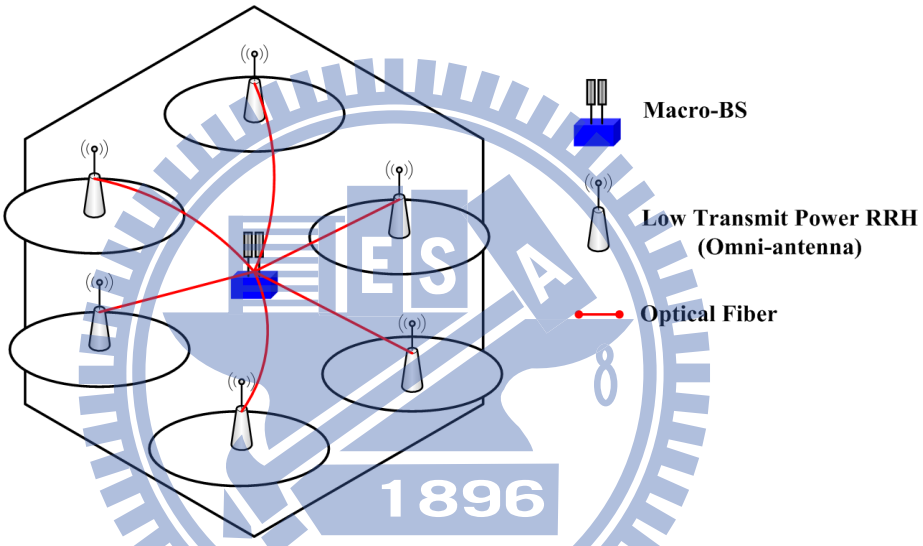

Figure 1.4: Scenarios 3 and 4: Network with low power RRHs within macro-BS coverage.

1.1 Problem and Feasible Solution

According to the previous work, we adopt JP transmission schemes in intra site in HetNet. The performance gain is limited since we do not consider the cooperation among macro-cells. In [3], it is advised that the hybrid category of JP and CS/CB may be possible. Therefore, we want to design a transmission approach which can combine intra- and inter-site coordination in HetNet [6]. We propose to jointly design a transmission scheme over scenarios 3 and 4. We proposed to further improve the system performance of both cell average and cell-edge throughput. In this thesis, we consider a joint transmission scheme of JP in intra-site and CS/CB in inter-site. We would like to examine whether the joint design of JP and CS/CB for HetNet is a feasible way to further improve the system performance of cell average and cell-edge throughput.

1.2 Thesis Outline

The next chapter is our background and related work of this thesis. In Chapter 3, we model the received signal model and formulate the problem about ICI in our signal model. In Chapter 4, a joint cooperation design of intra-site and inter-site is proposed, and the feedback requirement of different transmission schemes is analyzed. We evaluate the system performance of this proposal and other transmission schemes in Chapter 5. The final chapter is our conclusions about joint cooperation design, which can mitigate ICI efficiently and further improve the system performance.

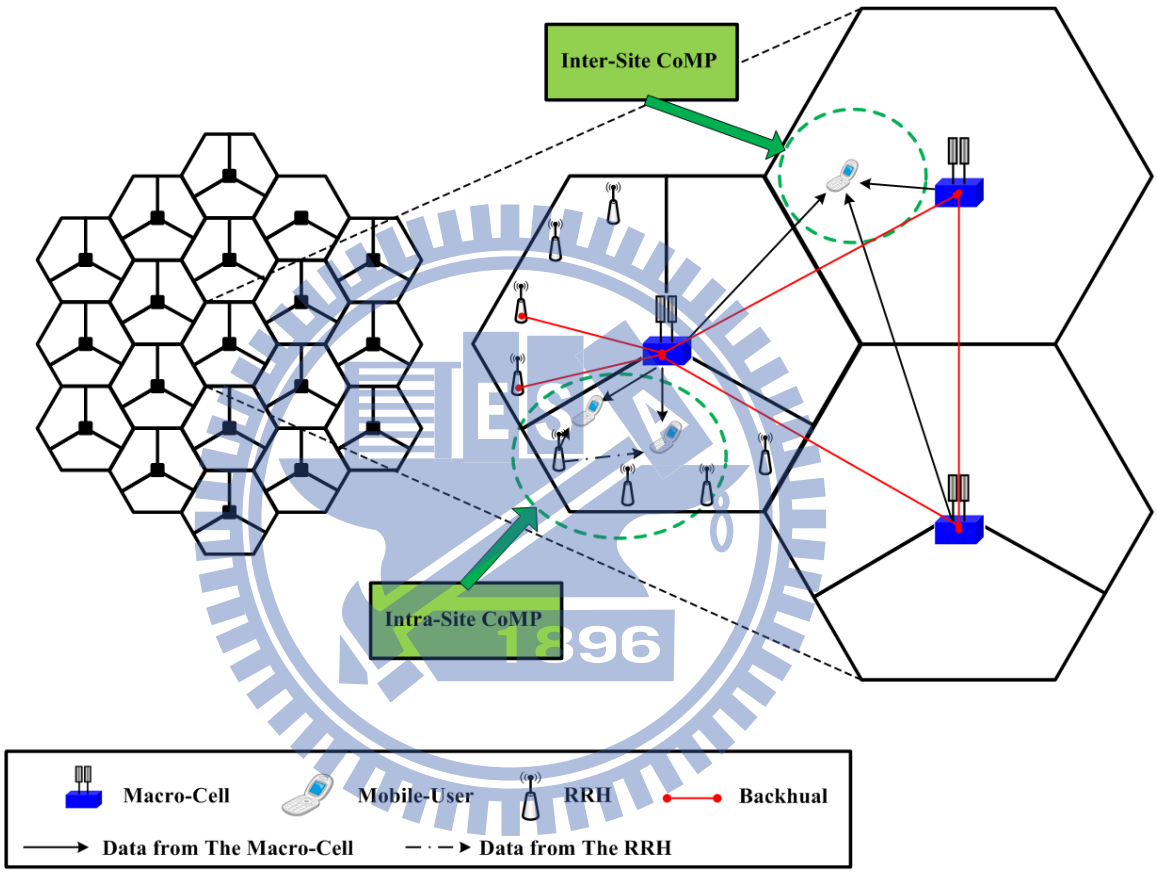

Figure 1.5: Intra- and inter-site CoMP region.

CHAPTER 2

Background

2.1 Literature Survey

The 3GPP has adopted orthogonal division multiple access (OFDMA) for the downlink transmission and single carrier frequency division multiple access (SC-FDMA) for the uplink transmission for LTE-A system. Furthermore, they conclude that cooperation among several cells can bring enormous gain in the spectrum efficiency. We investigate the transmission schemes operation in the downlink of LTE-A system. In the downlink case, we adopt the detailed time-frequency resource used in LTE-A systems. According to [7], we show the frame structure in Fig. 2.1.

CoMP transmission and reception is considered for the LTE-A as a tool to improve the coverage of high data rate, the cell-edge throughput, and to increase system throughput. We use CoMP techniques to mitigate the ICI and demonstrate the spectral efficiency in heterogeneous networks. Many researchers have already investigated different cooperative transmission schemes in four aforementioned scenarios. According to our previous work, we already operate the intra-site JP over 3GPP scenarios 3 and 4. We evaluate both cell average and cell-edge throughput. In scenario 3, each BS and RRH has its own reference signal set and resource for control signal channel for transmission and reception. With different cell IDs, they can assign the orthogonal frequency resource to cells which have different reference signals. In

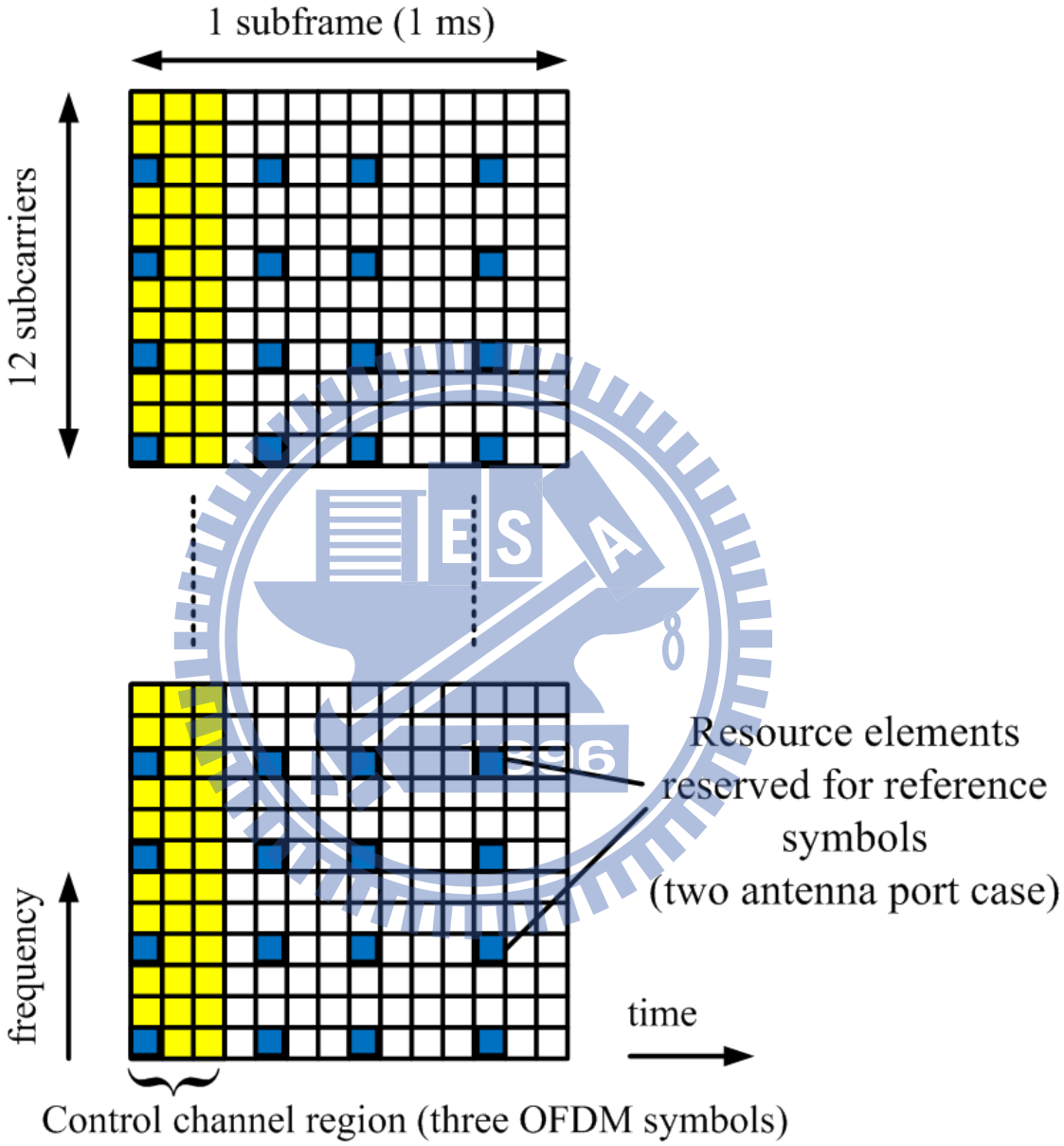

Figure 2.1: Time-frequency region used for downlink control.

Table 2.1: **Comparison of our work and other literatures.**

	HomoNet	HetNet	JP	CS/CB	Feedback delay	Joint Design	Cell architecture
[9]	√	×	√	√	√	×	×
[10]	√	√	√	√	×	×	×
Our Work	×	√	√	√	√	√	√

scenario 3 with JP, the collision will occur when macro-BS using different reference signal in a resource element. This will limit the provided gain. BS and RRHs have the same cell ID in scenario 4. With the same cell ID, JP can easily be applied by sharing transmission and reception control channel and reference signals. Since the BSs can exchange the information about channel from different BSs to different user equipments (UEs) through X2 interface. We use the cooperation between BSs in HetNet and extend the cooperation range.

Since there are backhaul connections among collaborative macro-BSs, we can extend the cooperative area from the intra-site to inter-site. On the other hand, we design a joint cooperation transmit approach to further improve the system performance. Because using three coordinated cells can outperform large number coordinated cells [8], we use three-cell coordinated network MIMO in the inter-site cooperation. We compare our work items with other existing work in Table 2.1.

2.2 LTE-A System-Level Simulator

From the previous work [11], we have already developed a LTE-A system-level simulator. In step 1a (for wideband SINR) and 1c (for spectral efficiency) [12, 13], our work is consistent with other existing simulation calibration results. Thus, the simulator is ready to simulate different advanced proposals.

CHAPTER 3

System Model and Problem Formulation

3.1 Cell Structures and Cellular MIMO Systems

Fig. 3.1 is the three types of cellular architectures recommended by 3GPP group.

1. *Diamond-shaped Wide beam Tri-sector Cell :* The diamond-shaped wide beam tri-sector cell is a conventional cellular architecture with three 120° directional antennas at each base station. The 3 dB power attenuation angle is set to 70°.

2. *Pentagonal Wide beam Tri-sector Cell :* The pentagonal wide beam tri-sector cell architecture is defined in the 3GPP LTE-A standard body [1]. It uses the 120° directional antennas, with the 3 dB power attenuation angle set to 70°. Compared with the diamond-shaped, the beam direction of pentagonal tri-sector cell is revolved by an angle to further avoid interference from neighboring sectors.

3. *Narrow Beam Tri-sector Cell :* The narrow beam tri-sector cell is defined as the coverage area of a base station with three directional antennas, each of which has a 60° beamwidth, and the 3 dB power attenuation angle is set to 30°. Compared with the wide beam tri-sector cell, the narrow beam tri-sector cell has more potential against ICI.

We consider all three cell architectures with different CoMP techniques and compare their results to investigate the effects of different system parameter. When only using

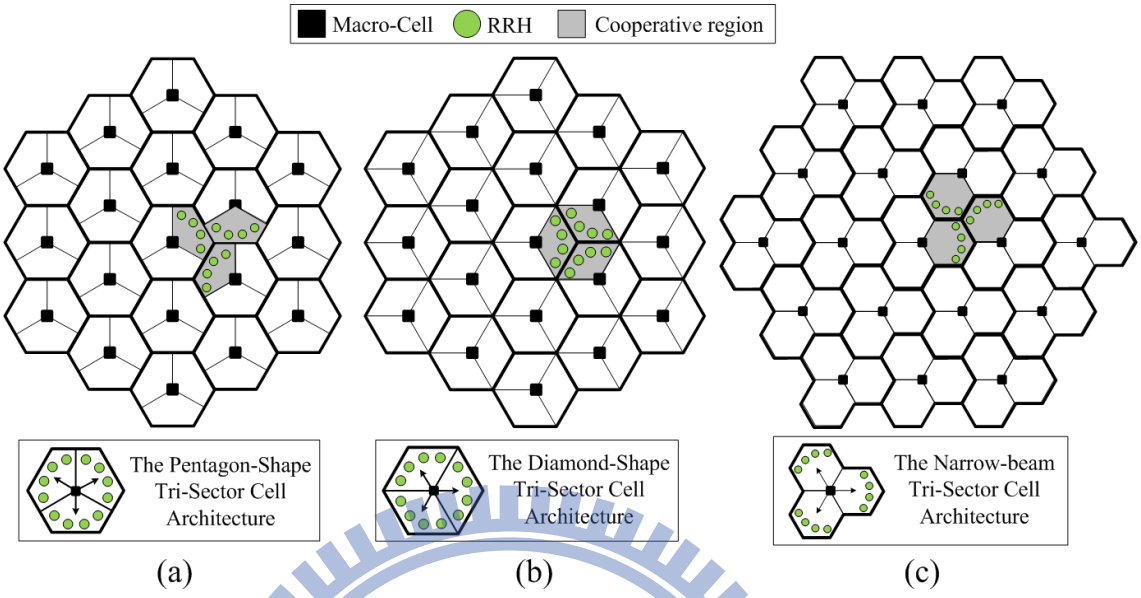

Figure 3.1: Three types of cell architectures.

the intra-site cooperation, the cell structures differences would not significantly affect the system performance. However, if we operate cooperation between BSs in inter-site, the cell structures would bring up some effects which can not be ignored.

Consider the cellular system environment consisting of 19 cells with hexagonal grid and each cell is divided into three sectors. Each sector is equipped with directional antenna, and there are N_t transmit antennas at each BS, N_r receive antennas at each UE, and total N_u UEs in each sector. In the wireless cellular environment, the UEs served by the macro-cell would be interfered by the other cells in the systems. Inter cell interference is a source of degradation to system performance and decrease the SINR. We assume there are N_t transmit antenna at BS and N_r receive antenna at UE. For the received signal and corresponding signal-to-interference-plus-noise ratio

(SINR) in a cellular system, we can formulate as equations below:

$$R_{b,s,u} = \underbrace{H_{b,s,u}W_{b,s,u}X_{b,s,u}}_{\text{desired signal}} + \underbrace{\sum\nolimits_{i\neq b} H_{i,j,k}W_{i,j,k}X_{i,j,k}}_{\text{inter-cell interference}} + n_{b,s,u} \tag{3.1}$$

$$SINR_{b,s,u} = \frac{\|M_{b,s,u}H_{b,s,u}W_{b,s,u}\|^2 \cdot P_{b,s,u}}{\sum_{i\neq b}\|M_{b,s,u}H_{i,j,k}W_{i,j,k}\|^2 \cdot P_{i,j,k} + \sigma_n^2} \tag{3.2}$$

where $H_{b,s,u} \in C^{N_t \times N_r}$ as channel matrix from the b^{th} BS to the u^{th} UE in the s^{th} sector. $W_{b,s,u}$ as corresponding weighting matrix for the u^{th} UE in the s^{th} sector of the b^{th} BS. $M_{b,s,u}$ as receiver matrix for the u^{th} UE in the s^{th} sector of the b^{th} BS. $P_{b,s,u}$ as the received power from the b^{th} BS to the u^{th} UE in the s^{th} sector. $n_{b,s,u} \in C^{N_t \times 1}$ is additive white Gaussian noise (AWGN) with $\sigma_n^2 = -174\frac{dBm}{Hz}$ power density. In a cellular system, we can design the weighting matrix to mitigate ICI and increase the system performance by CS/CB operation. For further suppressing ICI, we want to min $(M_{b,s,u}H_{i,j,k}W_{i,j,k})$.

3.2 Heterogeneous Network Systems Signal Model

In this section, we arrange some RRHs within macro-cell coverage, and two different types of RRH nodes are considered:

1. RRH nodes have the same cell ID as the corresponding macro-BS.
2. RRH nodes have different cell IDs from the corresponding macro-BS.

All the RRHs are connected to the macro-BS via a high speed backhaul (e.g. optical fiber). CSI and data from macro-BS and RRHs can be exchanged and cooperation between cells can be operated. When a macro-BS and RRHs operate JP-CoMP in intra-site and serve the same user, the effective channel can be detected by the user denotes as:

$$H_{c,s,u}^{eff} = H_{c,s,u} + \sum_{i=1}^{N} H_{c,s,u}^{RRH_i} \tag{3.3}$$

where $H^{eff}_{c,s,u} \in C^{N_t \times N_r}$ denotes effective channel. $H_{c,s,u}$ denotes channel from the c^{th} macro-cell's the s^{th} sector to the u^{th} user. $H^{RRH_i}_{c,s,u}$ denotes channel from the i^{th} RRH node within the c^{th} macro-cell in the s^{th} sector to the u^{th} user. Hence, we can formulate the received signal of the u^{th} user in the c^{th} macro-cell's the s^{th} sector as

$$R_{c,s,u} = \underbrace{H^{eff}_{c,s,u} W_{c,s,u} S_{c,s,u}}_{\text{desired signal}} + \underbrace{\sum_{i \neq c}^{N} H^{eff}_{i,j,k} W_{i,j,k} S_{i,j,k}}_{\text{inter-cell interference}} + n_{c,s,u} \tag{3.4}$$

where $S_{c,s,u}$ denotes the desired signal of the u^{th} user in the c^{th} macro-cell's the s^{th} sector. $W_{c,s,u}$ denotes the corresponding weighting matrix of the u^{th} user in the c^{th} macro-cell's the s^{th} sector. $n_{b,s,u} \in C^{N_t \times 1}$ is additive white Gaussian noise (AWGN) with $\sigma_n^2 = -174 \frac{dBm}{Hz}$ power density.

In the HetNet systems, a macro-BS and RRHs within its coverage can serve different users. Thus, the macro-users and RRH-users can suffer extra intra-cell interference from each other. The macro-user and RRH-user are served by corresponding BSs simultaneously, and the intra-user interference will degrade both users' spectrum efficiency. We adopt the network MIMO techniques. Since the macro-BS and RRHs are connected via a high speed backhaul, they can cooperate as a virtual MIMO system to jointly serve both macro-user and RRH-user. We assume that the u^{th} user is served by the c^{th} macro-BS and the t^{th} is served by the r^{th} RRH. The u^{th} user can detect the channel coming from the c^{th} macro-BS as $H_{c,s,u}$. Similarly, the t^{th} user can detect the channel coming from the r^{th} RRH as $H^{RRH}_{c,s,t}$. We regard these coordinated nodes as a virtual MIMO system, an effective combined channel matrix of the co-scheduled users can be respectively written as $H^{eff}_{c,s,u}$ and $H^{eff}_{c,s,t}$ where:

$$H^{eff}_{c,s,u} = \begin{bmatrix} H_{c,s,u} & H^{RRH}_{c,s,t} \end{bmatrix} \tag{3.5}$$

and

$$H^{eff}_{c,s,t} = \begin{bmatrix} H^{RRH}_{c,s,t} & H_{c,s,u} \end{bmatrix} . \tag{3.6}$$

Therefore, we rewrite the received signal of u^{th} macro-user and t^{th} RRH-user as follows

$$R_{c,s,u} = \underbrace{H^{eff}_{c,s,u} W_{c,s,u} X_{c,s,u}}_{\text{desired signal}} + \underbrace{H^{eff}_{c,s,t} W_{c,s,t} X_{c,s,t}}_{\text{intra-user interference}} + \underbrace{\sum_{i \neq c} H^{eff}_{i,j,k} W_{i,j,k} X_{i,j,k}}_{\text{inter-cell interference}} + n_{c,s,u} \tag{3.7}$$

where $X^{eff}_{c,s,u}$ is the desired signal of the u^{th} macro-user, $W_{c,s,u}$ is the corresponding precoding matrix, and $n_{c,s,u}$ is the additive white Gaussian noise with $\sigma_n^2 = -174\,\text{dBm/Hz}$ power density.

Similarly, the received signal of the t^{th} RRH-user can be formulated as:

$$R_{c,s,t} = \underbrace{H^{eff}_{c,s,t} W_{c,s,t} X_{c,s,t}}_{\text{desired signal}} + \underbrace{H^{eff}_{c,s,u} W_{c,s,u} X_{c,s,u}}_{\text{intra-user interference}} + \underbrace{\sum_{i \neq c} H^{eff}_{i,j,k} W_{i,j,k} X_{i,j,k}}_{\text{inter-cell interference}} + n_{c,s,t} \tag{3.8}$$

where $X_{c,s,t}$ is the desired signal of the t^{th} RRH-user, $W_{c,s,t}$ is the corresponding precoding matrix, and $n_{c,s,t}$ is the additive white Gaussian noise with $\sigma_n^2 = -174\,\text{dBm/Hz}$ power density.

3.3 Codebook-based Precoder

In the LTE-A system, a user cannot feedback whole channel state to the mcaro-BS because the feedback channel bandwidth is limited. As the LTE-A system, a codebook based precoder is applied in our simulation. Each user in LTE-A MIMO system can calculate the precoding matrix from the channel and feedback the index of codebook as PMI to the macro-BS. Since the same codebook set is designed offline and known at both the transmitter and receiver, users only feedback the PMI can reduce the overhead load obviously. Table 3.1 lists the codebook sets for two antenna ports are defined in [14].

Table 3.1: **Release 9 two antenna ports codebook.**

Index	**Rnak-1**	**Rnak-2**
$\mathbf{C}_0$	$\frac{1}{\sqrt{2}}\begin{bmatrix}1\\1\end{bmatrix}$	$\frac{1}{2}\begin{bmatrix}1 & 1\\1 & -1\end{bmatrix}$
$\mathbf{C}_1$	$\frac{1}{\sqrt{2}}\begin{bmatrix}1\\-1\end{bmatrix}$	$\frac{1}{2}\begin{bmatrix}1 & 1\\j & -j\end{bmatrix}$
$\mathbf{C}_2$	$\frac{1}{\sqrt{2}}\begin{bmatrix}1\\j\end{bmatrix}$	
$\mathbf{C}_3$	$\frac{1}{\sqrt{2}}\begin{bmatrix}1\\-j\end{bmatrix}$	

Table 3.2: **Release 9 Four Antenna Ports Codebook**

Index	$\mathbf{u}_c$	**Rank-1**	**Rank-2**
$\mathbf{C}_0$	$\mathbf{u}_0 = \begin{bmatrix} 1 & -1 & -1 & -1 \end{bmatrix}^{\mathrm{T}}$	$\mathbf{W}_0^1$	$\mathbf{W}_0^{1,4}/\sqrt{2}$
$\mathbf{C}_1$	$\mathbf{u}_1 = \begin{bmatrix} 1 & -j & 1 & j \end{bmatrix}^{\mathrm{T}}$	$\mathbf{W}_1^1$	$\mathbf{W}_1^{1,4}/\sqrt{2}$
$\mathbf{C}_2$	$\mathbf{u}_2 = \begin{bmatrix} 1 & 1 & -1 & 1 \end{bmatrix}^{\mathrm{T}}$	$\mathbf{W}_2^1$	$\mathbf{W}_2^{1,4}/\sqrt{2}$
$\mathbf{C}_3$	$\mathbf{u}_3 = \begin{bmatrix} 1 & j & 1 & -j \end{bmatrix}^{\mathrm{T}}$	$\mathbf{W}_3^1$	$\mathbf{W}_3^{1,2}/\sqrt{2}$
$\mathbf{C}_4$	$\mathbf{u}_4 = \begin{bmatrix} 1 & (-1-j)/\sqrt{2} & -j & (1-j)/\sqrt{2} \end{bmatrix}^{\mathrm{T}}$	$\mathbf{W}_4^1$	$\mathbf{W}_4^{1,4}/\sqrt{2}$
$\mathbf{C}_5$	$\mathbf{u}_5 = \begin{bmatrix} 1 & (1-j)/\sqrt{2} & j & (1-j)/\sqrt{2} \end{bmatrix}^{\mathrm{T}}$	$\mathbf{W}_5^1$	$\mathbf{W}_5^{1,4}/\sqrt{2}$
$\mathbf{C}_6$	$\mathbf{u}_6 = \begin{bmatrix} 1 & (1+j)/\sqrt{2} & -j & (-1+j)/\sqrt{2} \end{bmatrix}^{\mathrm{T}}$	$\mathbf{W}_6^1$	$\mathbf{W}_6^{1,3}/\sqrt{2}$
$\mathbf{C}_7$	$\mathbf{u}_7 = \begin{bmatrix} 1 & (-1+j)/\sqrt{2} & j & (1+j)/\sqrt{2} \end{bmatrix}^{\mathrm{T}}$	$\mathbf{W}_7^1$	$\mathbf{W}_7^{1,3}/\sqrt{2}$
$\mathbf{C}_8$	$\mathbf{u}_8 = \begin{bmatrix} 1 & -1 & 1 & 1 \end{bmatrix}^{\mathrm{T}}$	$\mathbf{W}_8^1$	$\mathbf{W}_8^{1,2}/\sqrt{2}$
$\mathbf{C}_9$	$\mathbf{u}_9 = \begin{bmatrix} 1 & -j & -1 & -j \end{bmatrix}^{\mathrm{T}}$	$\mathbf{W}_9^1$	$\mathbf{W}_9^{1,4}/\sqrt{2}$
$\mathbf{C}_{10}$	$\mathbf{u}_{10} = \begin{bmatrix} 1 & 1 & 1 & -1 \end{bmatrix}^{\mathrm{T}}$	$\mathbf{W}_{10}^1$	$\mathbf{W}_{10}^{1,3}/\sqrt{2}$
$\mathbf{C}_{11}$	$\mathbf{u}_{11} = \begin{bmatrix} 1 & j & -1 & j \end{bmatrix}^{\mathrm{T}}$	$\mathbf{W}_{11}^1$	$\mathbf{W}_{11}^{1,3}/\sqrt{2}$
$\mathbf{C}_{12}$	$\mathbf{u}_{12} = \begin{bmatrix} 1 & -1 & -1 & 1 \end{bmatrix}^{\mathrm{T}}$	$\mathbf{W}_{12}^1$	$\mathbf{W}_{12}^{1,2}/\sqrt{2}$
$\mathbf{C}_{13}$	$\mathbf{u}_{13} = \begin{bmatrix} 1 & -1 & 1 & 1- \end{bmatrix}^{\mathrm{T}}$	$\mathbf{W}_{13}^1$	$\mathbf{W}_{13}^{1,3}/\sqrt{2}$
$\mathbf{C}_{14}$	$\mathbf{u}_{14} = \begin{bmatrix} 1 & 1 & -1 & -1 \end{bmatrix}^{\mathrm{T}}$	$\mathbf{W}_{14}^1$	$\mathbf{W}_{14}^{1,3}/\sqrt{2}$
$\mathbf{C}_{15}$	$\mathbf{u}_{15} = \begin{bmatrix} 1 & 1 & 1 & 1 \end{bmatrix}^{\mathrm{T}}$	$\mathbf{W}_{15}^1$	$\mathbf{W}_{15}^{1,2}/\sqrt{2}$

Because rank-1 and rank-2 transmission schemes can be adopted for two transmission antenna, we take two types of codebook sets. For rank-1 and rank-2 transmission, four code words, i.e., C_0,C_1,...,C_3, are listed in Table 3.1.

According to [15,16], we calculate the precoding matrix by using the dominant eigen mode. In case of $N_t \geq N_r$, we need to decompose the channel $H_{c,s,u}$ of the u^{th} user in the c^{th} macro-cell's the s^{th} sector by using singular value decomposition (SVD). We regard the leftmost column $V_{c,s,u}$ as the full precoding matrix and this can guarantee that we transmit our signal with better channel quality. For SU-MIMO rank-1 and rank-2 transmission, we take $v^1_{c,s,u}$ and $\begin{bmatrix} v^1_{c,s,u} & v^2_{c,s,u} \end{bmatrix}$ as the full precoding matrix of rank-1 and rank-2 respectively, i.e., the full precoding matrix $\hat{W}_{c,s,u}$. After calculating the full precoding matrix, we map it to the codebook set to search a most suitable codeword [17] [18]. Codeword can be chosen by the minimum angle between candidate codeword and the full precoding matrix.

$$index = \arg\max trace\left(\left|C_i^H \hat{W}_{c,s,u}\right|\right) \tag{3.9}$$

where C_i is from codebook set defined in the previous table. Index is the rank indicator of the selected codeword. By only feeding the index of the corresponding codeword back, a few feedback bits need to be transmitted and the overhead load can be reduced.

3.4 Receiver Structure and MIMO Switching

At receiver end, two types receiver structure are adopted for rank-1 and rank-2 transmission,which are maximal ratio combining (MRC) and minimum mean square error (MMSE) structures [1,19]. The MRC receiver can maximize the desired receive power in the single-user multiple-input multiple-output (SU-MIMO) system for rank-1 transmission. The MMSE receiver can be used for suppressing inter-stream and inter-user

interference for rank-2 transmission, where the former is caused by multi-stream in SU-MIMO and the latter is caused by multi-user in MU-MIMO system. Assuming the precoding vector $W_{c,s,u} = w^1_{c,s,u}$ is selected form codebook set, and we formulate the received signal as the following equation:

$$R_{c,s,u} = \underbrace{H_{c,s,u} w^1_{c,s,u} s^1_{c,s,u}}_{\text{desired signal}} + \underbrace{\sum_{i \neq c}^{N} H_{i,j,k} W_{i,j,k} S_{i,j,k}}_{\text{inter-cell interference}} + n_{c,s,u} \ . \tag{3.10}$$

The MRC receiver algorithm $M^1_{c,s,u} \in C^{1 \times N_r}$ for the u^{th} user in the c^{th} macro-cell's the s^{th} sector can be denoted as

$$M^1_{c,s,u} = \left[H_{c,s,u} w^1_{c,s,u} \right]^H . \tag{3.11}$$

We can use $M^1_{c,s,u}$ to demodulate the received signal by multiplying it by $R_{c,s,u}$ and get data symbol $s^1_{c,s,u}$.

In rank-2 SU-MIMO systems, the data symbols can be written as $S_{c,s,u} = \left[s^1_{c,s,u} \, s^2_{c,s,u} \right]$. Let the precoding matrix be $W_{c,s,u} = \begin{bmatrix} w^1_{c,s,u} & w^2_{c,s,u} \end{bmatrix}$, which are selected from codebook set. We formulate the received signal as

$$R_{c,s,u} = H_{c,s,u} \begin{bmatrix} w^1_{c,s,u} & w^2_{c,s,u} \end{bmatrix} \begin{bmatrix} s^1_{c,s,u} & s^2_{c,s,u} \end{bmatrix}^T + \sum_{i \neq c} H_{i,j,k} W_{i,j,k} S_{i,j,k} + n_{c,s,u} \ . \tag{3.12}$$

We derive the MMSE receiver algorithm, and $M^1_{c,s,u} \in C^{1 \times N_r}$ and $M^2_{c,s,u} \in C^{1 \times N_r}$ for the u^{th} user in the c^{th} macro-cell's the s^{th} sector can be denoted as

$$M^1_{c,s,u} = \left[\left((\sigma_n^2 I) + H_{c,s,u} w^2_{c,s,u} \left(H_{c,s,u} w^2_{c,s,u} \right)^H \right)^{-1} H_{c,s,u} w^1_{c,s,u} \right]^H \tag{3.13}$$

and

$$M^2_{c,s,u} = \left[\left((\sigma_n^2 I) + H_{c,s,u} w^1_{c,s,u} \left(H_{c,s,u} w^1_{c,s,u} \right)^H \right)^{-1} H_{c,s,u} w^2_{c,s,u} \right]^H \tag{3.14}$$

where we can use $M^1_{c,s,u}$ and $M^2_{c,s,u}$ for demodulating data symbols $s^1_{c,s,u}$ and $s^2_{c,s,u}$ by multiplying received signal $R_{c,s,u}$ by $M^1_{c,s,u}$ and $M^2_{c,s,u}$, respectively.

In the rank-1 MU-MIMO system, a BS with $N_t = 2$ can serve two users simultaneously with $N_r = 2$. These co-scheduled users can receive one data stream respectively. Here, we assume two users are in the s^{th} sector and served by the c^{th} cell, which are the u^{th} and the t^{th} user. Let $w^1_{c,s,u}$ be the selected precoding vector for the u^{th} user and $w^1_{c,s,t}$ is for the t^{th} user. And each data symbol, $x^1_{c,s,u}$ is for the u^{th} user and $x^1_{c,s,t}$ is for the t^{th} user. We can rewrite the received signal equation as follows

$$R_{c,s,u} = H_{c,s,u}w^1_{c,s,u}x^1_{c,s,u} + \underbrace{H_{c,s,t}w^1_{c,s,t}x^1_{c,s,t}}_{\text{inter-user interference}} + \underbrace{\sum_{i\neq c} H_{i,j,k}W_{i,j,k}X_{i,j,k}}_{\text{inter-cell interference}} \tag{3.15}$$

and

$$R_{c,s,t} = H_{c,s,t}w^1_{c,s,t}x^1_{c,s,t} + \underbrace{H_{c,s,u}w^1_{c,s,u}x^1_{c,s,u}}_{\text{inter-user interference}} + \underbrace{\sum_{i\neq c} H_{i,j,k}W_{i,j,k}X_{i,j,k}}_{\text{inter-cell interference}} . \tag{3.16}$$

We use the MMSE algorithm to derive our receiver matrix $M^1_{c,s,u} \in C^{1\times N_r}$ and $M^1_{c,s,t} \in C^{1\times N_r}$ for the u^{th} user and the t^{th} user as follows

$$M^1_{c,s,u} = \left[\left(\sigma_n^2 \mathrm{I} + H_{c,s,u}w^1_{c,s,t}\left(H_{c,s,u}w^1_{c,s,t}\right)^H\right)^{-1} H_{c,s,u}w^1_{c,s,u}\right]^H \tag{3.17}$$

and

$$M^1_{c,s,t} = \left[\left(\sigma_n^2 \mathrm{I} + H_{c,s,t}w^1_{c,s,u}\left(H_{c,s,t}w^1_{c,s,u}\right)^H\right)^{-1} H_{c,s,t}w^1_{c,s,t}\right]^H \tag{3.18}$$

where $M^1_{c,s,u}$ and $M^1_{c,s,t}$ are used to demodulate the data symbol $x^1_{c,s,u}$ and $x^1_{c,s,t}$ by multiplying the received signal $R_{c,s,u}$ and $R_{c,s,t}$, respectively.

Transmission rank adaptation should be adopted to increase spectrum efficiency of performance in the 3GPP LTE-A MIMO system [20, 21]. In SU-MIMO systems, we calculate both performance of rank-1 and rank-2 and choose one, which can yield the better spectrum efficiency and adopt the transmission rank. Since the

spatial multiplexing for higher rank can significantly improve performance, each user are supposed to determine the transmission rank and feedback to BS.

MU-MIMO is an advanced technology to enhance the spectrum efficiency. A BS here can serve multiple users (co-scheduled) in the same resource block by exploiting degrees of freedom in the spatial domain, and this can depend on the number of antennas at transmitter and receiver. Any users pair can not always be co-scheduled perfectly because of the CSI. Namely, when users whose CSIs are sufficiently orthogonal to each other in the MU-MIMO system are suitable to be co-scheduled. To enhance spectrum efficiency, a switching mode between SU and MU-MIMO is prerequisite [22–24]. In [22], it is shown that we can have approximate 21% performance gain as compared with the SU-MIMO systems by applying the SU/MU-MIMO switching techniques. Thus, we adopt the ideal SU/MU-MIMO switching techniques in our simulation.

3.5 Proportional Fair Scheduling

We try to guarantee that users in the center or at the cell edge can be served more fairly, we have to ensure that cell-edge users can also get the enough resources. Proportional fair scheduling can ensure the fairness of resources allocation and good transmission rate of cells. By applying proportional fair scheduling, we can avoid allocating resources always to the users who have the better transmission rate. The users can be served when the current transmission rate is higher or the past average transmission rate is lower. We consider both the current and the past average transmission rate of each users, and allocate resources as follows

$$s_b^{th} = \arg\max \left(\frac{R_{b,u,r}^c}{T_{b,u,r}^p} \right), u = 1, 2, ..., N_u \tag{3.19}$$

where $R^c_{b,u,r}$ denotes the current transmission rate of the u^{th} user served by the b^{th} BS in the r^{th} resource block (RB), $T^p_{b,u,r}$ denotes the past average transmission rate of the u^{th} user served by the b^{th} BS before the r^{th} RB, and the s^{th}_b is the index denotes the s^{th}_b user is selected to be served by the b^{th} BS in the r^{th} RB. By adopting proportional fair scheduling, we can ensure that both cell-center and cell-edge users can have the RBs to transmit.

3.6 Exponential Effective SINR Mapping (EESM)

Exponential Effective SINR Mapping is a method to map the instantaneous SINR to the corresponding block error rate (BLER) value. EESM can map the SINR of every subcarrier to an effective SINR by an equation below:

$$\gamma_{eff} = EESM(\gamma, \beta) = -\beta \ln \left(\frac{1}{N_c} \sum_{i=1}^{N_c} e^{-\frac{\gamma_i}{\beta}} \right) \tag{3.20}$$

where γ_i is the SINR of i^{th} subcarrier and N_c is the number of subcarrier per subband. Fifteen different modulation and coding scheme (MCS) corresponding to fifteen different CQI are defined in [25]. The effective SINR can be mapped to an MCS by SINR-BLER curve by link level simulator [26]. We choose the highest MCS with BLER not exceeding 0.1.

3.7 Hybrid Automatic Repeat Request (HARQ)

Since we provide a system level simulator, we did not include the link level behavior in our simulation. Thus, we model the transmission error by introducing a random variable with probability mass function (PMF) [11]:

$$P(X) = \begin{cases} 0.1\,, & x = 0 \\ 0.9\,, & x = 1 \end{cases} \tag{3.21}$$

where $x = 0$ denotes as the current transmission error, and $x = 1$ denotes as the successful transmission. If error occurs, we will retransmit again in the next transmission time interval (TTI). Suppose that we have a throughput T before considering transmission error. We formulate the relation between UE's throughput T_{UE} and retransmission time N_r as

$$T_{UE} = \frac{T}{(1 + N_r)} \tag{3.22}$$

where $0 \leq N_r \leq 3$. When transmission error occurs too many times, the throughput will be lower. If the transmission time is longer than three, the data will be discarded and the throughput of that TTI will be zero.

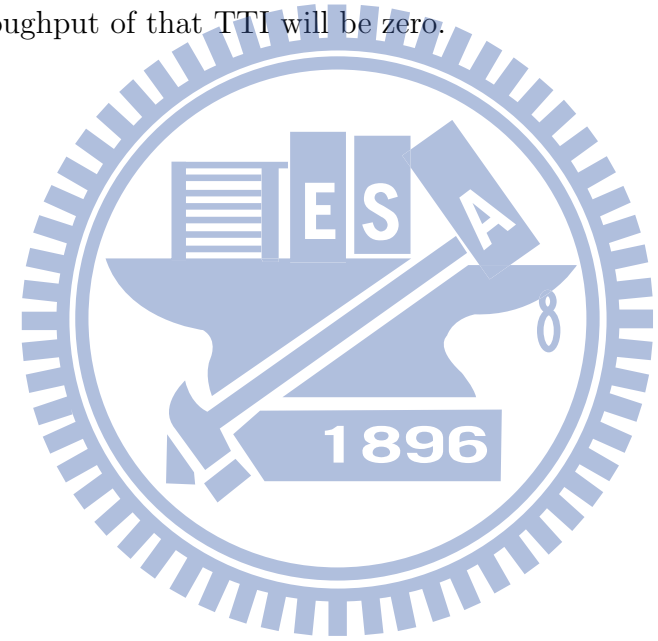

CHAPTER 4

Joint Cooperation Design in Both Intra- and Inter-Site CoMP

4.1 Coherent Intra-Site Joint Transmission

According to our previous work, we only use cooperation among macro-cells and RRHs with CoMP-JP in intra-site. In [3], we can further improve the performance by coherent JP. Coherent JP can compensate the RRH's channel by more information components about the channel. We use inter-point phase information to compensate the channel from RRH to the served UE and make the RRHs channel combined with macro-cells more precisely. As shown in Fig. 4.1, a user is served by a macro-BS and RRH at the same time. The overall channel matrix is as follow

$$H_{total}^{eff} = H_{macro} + \sum_{i=1}^{N} H_{i^{th}RRH} e^{j(\theta_{macro} - \theta_i)} \tag{4.1}$$

where H_{total}^{eff} is the effective channel matrix from the macro-cell combined with RRH's to the UE. H_{macro} is the channel matrix from macro-cell. $H_{i^{th}RRH}$ is the channel matrix from the i^{th} RRH. N is the number of cooperative RRHs. Because the channel's phase is compensated by the feedback component of phase information, we can use coherent intra-site JP, and the performance is better than non-coherent JP.

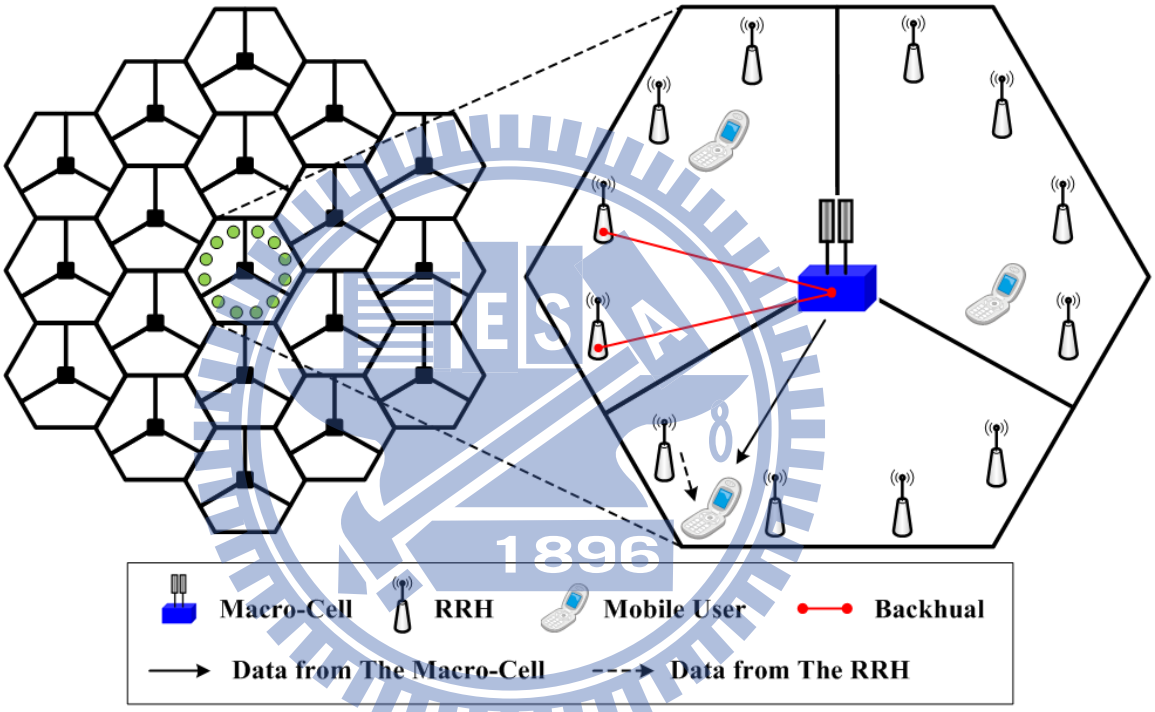

Figure 4.1: Coherent JP with phase compensation.

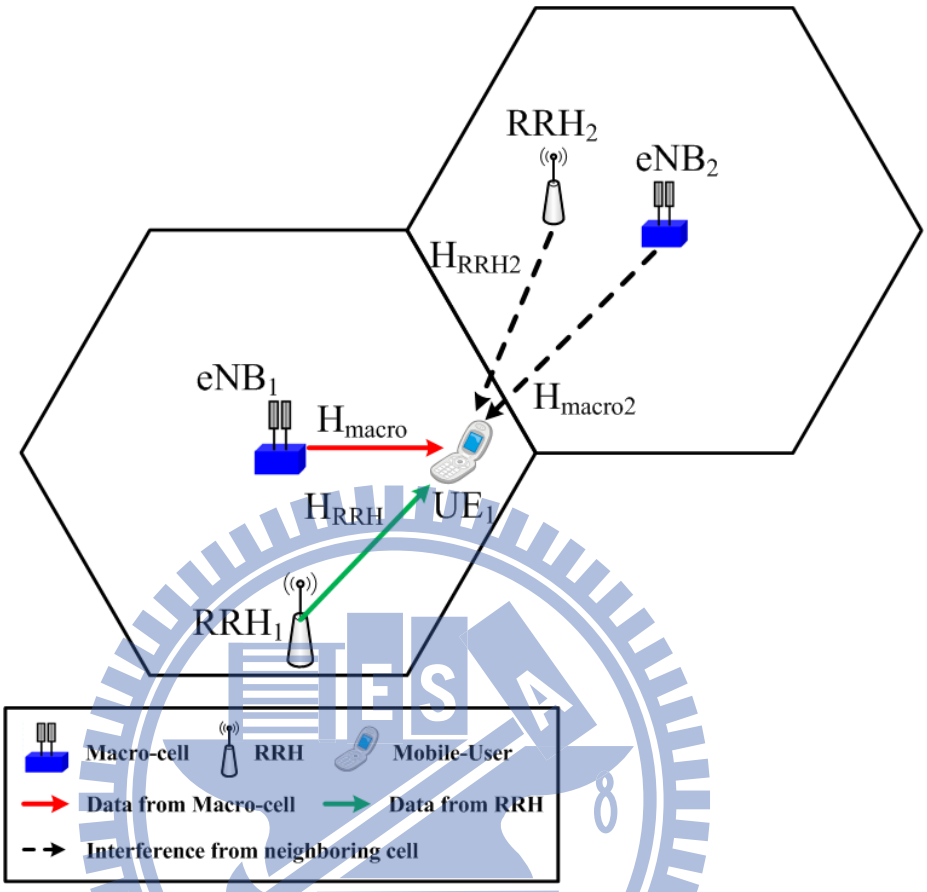

Figure 4.2: Two macro-cells wireless environment.

4.2 Inter-site Coordination Beamforming

Intra-site JP in can increase the received signal power. However, CoMP-CS/CB can effectively mitigate ICI. Through X2 interface, macro-cell cooperation can exchange the PMI. CS/CB techniques are accomplished by using the least interference PMI. An example of two cells environment is shown in Fig. 4.2 for CoMP-CS/CB in inter-site.

We assume that there are N_t transmit antenna at BS and N_r receive antenna

at UE and formulate the received signal as follows

$$R_1 = \underbrace{H_1 W_1 S_1}_{\text{desired signal}} + \underbrace{H_2 W_2 S_2}_{\text{inter-cell interference}} + n_1 \tag{4.2}$$

where $H_{ij} \in C^{N_t \times N_r}$ is the channel matrix form the i^{th} BS to the j^{th} user. $H_1 = H_{macro} + H_{RRH}$. $H_2 = H_{macro2} + H_{RRH2}$. W_j is weighting matrix of the j^{th} user. M_j is receiver matrix of the j^{th} user. P_{ij} is the received power from the i^{th} BS to the j^{th} user. $n_i \in C^{N_t \times 1}$ is additive white gaussian noise (AWGN) with $\sigma_n^2 = -174 \frac{dBm}{Hz}$ power density. Here, we try to make $H_2 W_2 = 0$. If the ICI can be completely mitigated, the only interference left will be the AWGN. We will have the maximum received SINR. For the two cells case, the SINR can be formulated as the following equation:

$$SINR_1 = \max \left(\frac{\|M_1 H_1 W_1\|^2 \cdot P_1}{\|M_1 H_2 W_2\|^2 \cdot P_2 + \sigma_n^2} \right). \tag{4.3}$$

However, no existing matrix W_2 can be multiplied by H_2 is exactly zero. We choose the weighting matrix which can make the interference be orthogonal to the desired signal. When the received signal is multiplied by the receive matrix, we can mitigate the ICI. We choose a codeword from the codebook set W_{set} , and the SU-MIMO can use multiple rank transmission by calculating the equation below:

$$W_2 = \min \left(\left| H_1 W_1 (H_2 W_j)^H \right| \right), \forall W_j \in W_{rank1-set} \tag{4.4}$$

$$W_2 = \min \left(tr \left(H_1 W_1 (H_2 W_j)^H \right) \right), \forall W_j \in W_{rank2-set} \tag{4.5}$$

ICI component can be mitigated with multiplying the received signal with MMSE receive matrix, which is derived by selected precoding weighting matrix. Because the inter-cell interference is orthogonal to the desired signal, we can maximize the received SINR, which is represented by

$$SINR_1 = \frac{\|M_1 H_1 W_1\|^2 \cdot P_1}{\|M_1 H_2 W_2\|^2 \cdot P_2 + \sigma_n^2} \ . \tag{4.6}$$

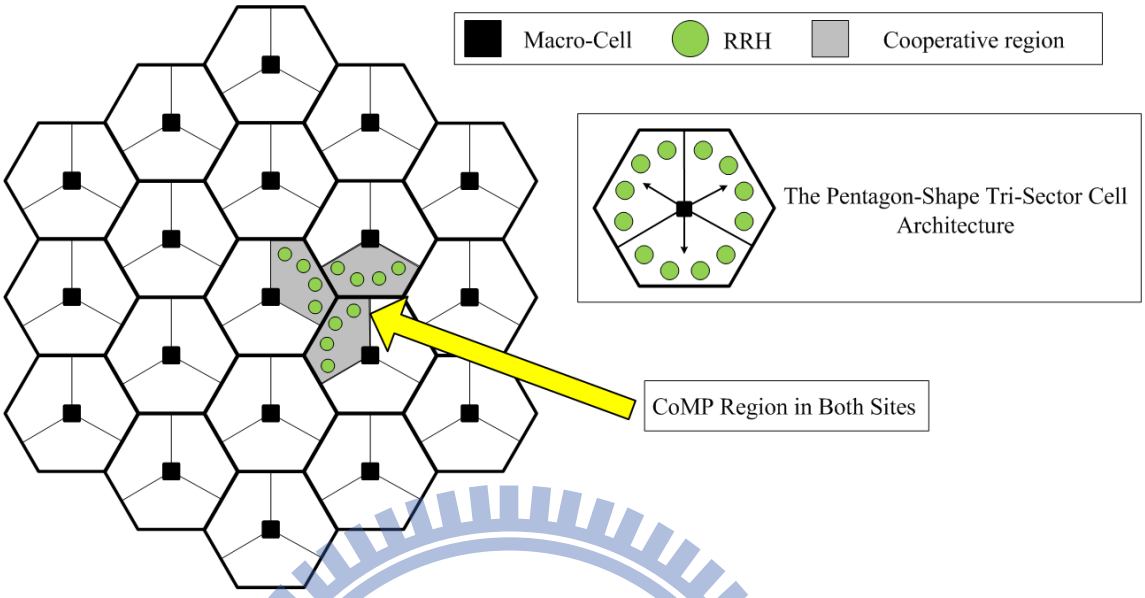

Figure 4.3: CoMP region over intra and inter-site.

We only need to exchange the index of orthogonal PMI among cooperation macro-BSs. Moreover, choosing the UEs served by BS2 in the cooperative area by proportional fair scheduling can maintain the cell average and cell-edge throughput. If the cooperation set is larger, we can calculate the coordinating precoding matrix by the same steps. We use three cells as a coordinated set in our simulations.

4.3 Joint Cooperation Design of Inter- and Intra-Site

We propose to combine the intra and inter-site CoMP and extend the CoMP region in Fig. 4.3. We present the joint cooperation design and a flow chart of this proposal in Fig. 4.4 as the following steps.

Step 1 : Estimate the combined channel from macro-cell and RRH : H_1 =

$H_{macro} + H_{RRH}$.

Step 2 : Estimate the interference channel : $H_2 = H_{macro2} + H_{RRH2}$.

Step 3 : Calculate the precoding matrix W_1 based on H_1.(used by eNB_1)

Step 4 : Calculate the coordinated precoding matrix W_2 for minimizing the inter-cell interference.(used by eNB_2)

$$\begin{cases} W_{2-rank1} = \min\left((H_1 W_1)^H H_2 W_j \right), \forall W_j \in W_{rank1-set} \\ W_{2-rank2} = \min\left(tr\left((H_1 W_1)^H H_2 W_j \right) \right), \forall W_j \in W_{rank2-set} \end{cases} \tag{4.7}$$

CoMP-JP in both the intra and inter-site needs to share all data and CSIs to multiple cells. It will take more time to exchange all the information. Compared with CoMP-JP in both intra and inter-site, our approach only needs to feedback information of orthogonal PMI in inter-site to the collaborative cells.

4.4 Impact of Feedback Requirement and Delay

When we operate CoMP-JP in intra-site, we need more feedback components to use coherent CoMP-JP, such as inter-point phase information and aggregated CSI. Compared with the MIMO systems, the feedback components are more in CoMP systems. Fig. 4.5 shows the feedback components differences between SU-MIMO transmission and coherent CoMP-JP. Since more components need to be measured, it will take more time to complete the feedback information reception, which leads to channel state changes.

Under our consideration, we use CoMP-JP in intra-site and CS/CB in inter-site to further improve the spectrum efficiency. We list the necessary feedback components of different CoMP schemes in Fig. 4.5. By our approach, we need the index of PMI to coordinated sectors as coordinated PMI (C-PMI) and delta-CQI when neighboring cells use C-PMIs. The aggregated RI, PMI, and CQI are measured for CoMP-JP in

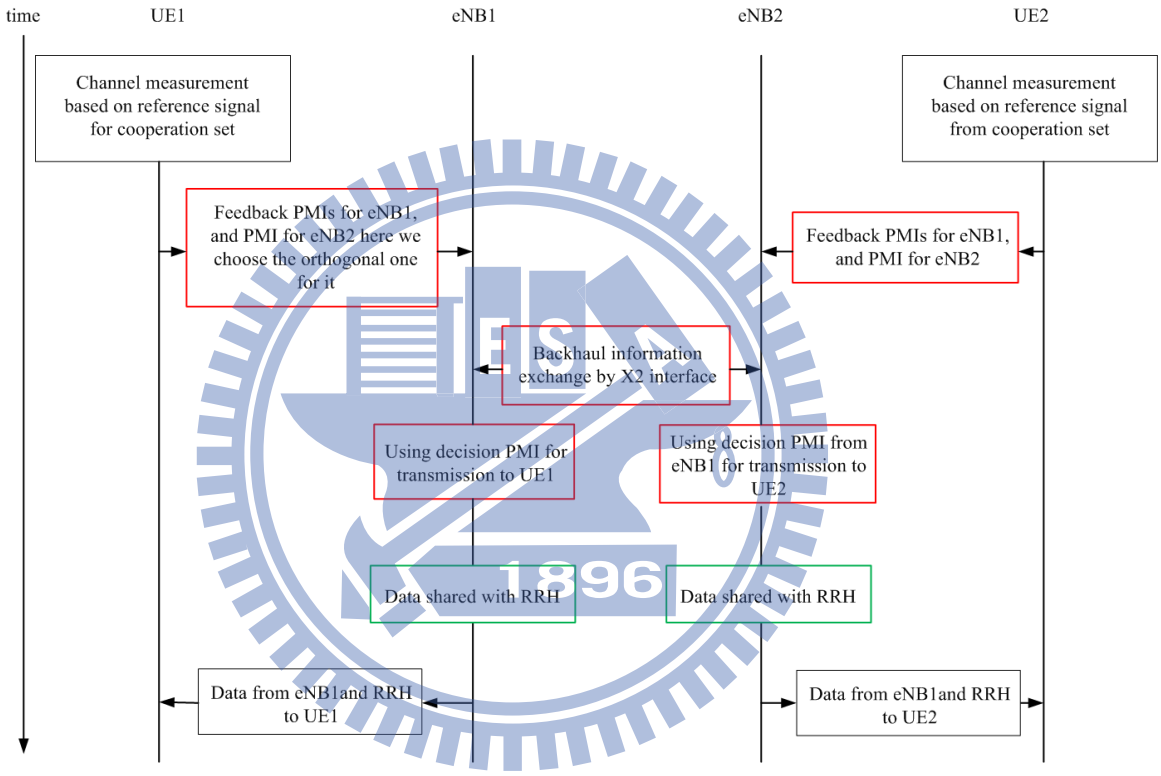

Figure 4.4: Flowchart of joint cooperation design.

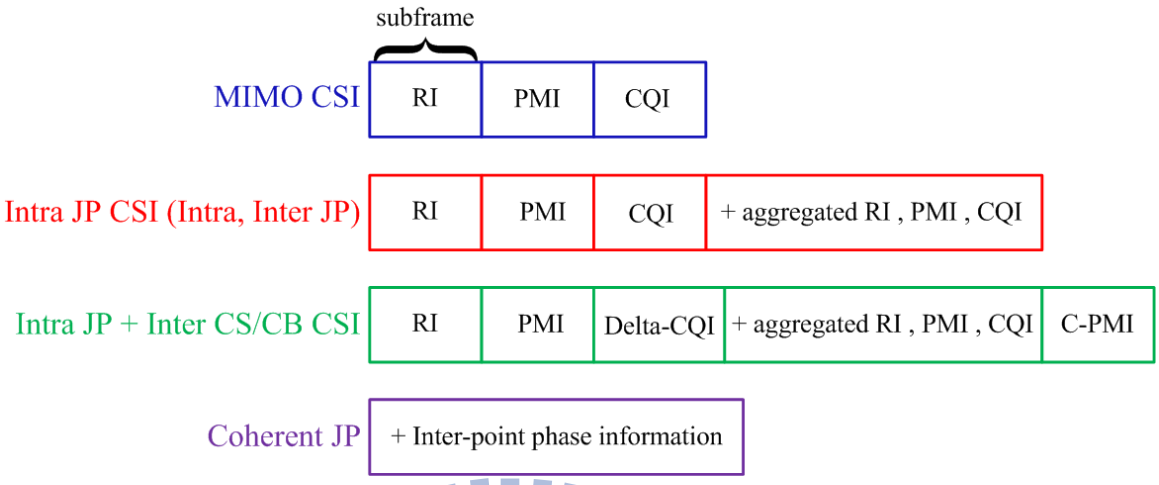

Figure 4.5: Feedback components comparison.

intra-site. We simulate the feedback delay impact of spectrum efficiency for different CoMP schemes.

CHAPTER 5

Numerical Results and Discussion

5.1 Parameters Setting of LTE-A System

In this section, we evaluate performance of several CoMP transmission schemes and compare their results. Fig. 5.1 shows a flow chart of our simulation procedures.

Our simulation environment is based on 3GPP standard [1], where the center frequency is 2 GHz; inter site distance (ISD) is 500 meters; downlink bandwidth is 10 MHz; penetration loss is 20 dB; and user speed is 3 km/hr. There are nineteen cell sites with the hexagonal grid in this cellular system, and each cell in this cellular system is divided into three sectors. All the cell sites work on the same frequency band, and frequency division duplex transmission mode is adopted. Channel model is urban-macro spatial channel model with high spread, and maximum retransmission times is four. The simulation parameters for MIMO system are listed as Table 5.1.

Since our simulation is over heterogeneous networks, we add four RRHs in every sector. Each RRH has two transmit antenna and transmit power is 30 dBm; omni-antennas are used; moreover, pathloss model is $128.1 + 37.6 \log_{10}(d)$, where d is in kilometers. The proportional fair scheduling and rank adaptation technique are also adopted in the simulation. The minimum distance is restricted as Fig. 5.2, which is applicable to all channel models.

5.2 Joint Cooperation Design Simulation Results Analysis

Simulation results of different CoMP schemes in both the intra and inter-site are provided in this section. The average throughput of SU-MIMO in the entire cell and at the cell edge is 2.39 (bps/Hz/cell) and 0.0791 (bps/Hz/user), respectively. We regard the performance of SU-MIMO as a baseline and compare it with different CoMP schemes in Figs. 5.3 and 5.4. When adopting JP in the intra-site technique with RRH location in 0.6R (R is the cell radius), spectrum efficiency improve 23%. The proposed scheme intra-JP and inter-CS/CB scheme can further improve spectrum efficiency by 41.7% at the cell edge and 15% in the entire cell. Thus, the proposed joint design of CoMP transmission scheme can effectively mitigate the ICI on average.

According to our previous work, we provide the performance of MU-MIMO in cell edge and cell average, which are 0.086 bps/Hz/user and 2.62 bps/Hz/cell. In Figs. 5.5 and 5.6, the SU/MU-MIMO switching techniques are adopted. Since the serving cell can connect multiple users in the same resource block by exploiting the degrees of freedom in the spatial domain, MU-MIMO can achieve higher throughput than only adopting SU-MIMO. As shown in Figs. 5.5 and 5.6, the proposed scheme can achieve additional gain of 54.65% and 19.32% in cell edge and cell average compared to the inter-JP CoMP. As compared with SU-MIMO, the proposed joint design, we can have relative gain of 100.63% and 61.24%, which is very significant.

We consider the effect of cell architectures on SU-MIMO and CoMP schemes. Figs. 5.7 and 5.8 show that the narrow-beam tri-sector architecture is the most suitable scheme for CoMP intra-JP plus inter-CS/CB scheme. Since the narrow beam tri-sector cell has more potential against ICI, the narrow-beam tri-sector can provide the users better performance than others. When users are located at cell edge and the angle is over 3 dB power attenuation angle, the cell-edge users can still be

served by macro-cell and RRHs. Compared with pentagonal, the proposed scheme has performance gain of 8% and 3.32% in cell edge and cell average, respectively.

In Figs. 5.9 and 5.10, phase compensation techniques can further enhance the performance of three different CoMP schemes, especially for inter-JP plus intra-JP transmission scheme. Compared to SU-MIMO, the proposed CoMP joint design technique improves performance of 71.6% and 49% in the cell edge and cell average, respectively. We listed the performance of three different CoMP schemes in Table 5.11. Based on [3], the feedback delay of 20 msec will degrade the system performance by 5% and 10% in cell average and cell edge, respectively. As shown in Table 5.11, our results can match the results provided by the 3GPP standard.

We use different transmission schemes in this chapter to show that the joint cooperation design can outperform other existing methods. In this section, we compare the performance of intra-site JP combined with inter-site CS/CB and inter and intra-site JP. The former transmission scheme is more efficient than the latter. We suggest that when operating CoMP techniques in both sites, the best combination method is the intra-site JP and the inter-site CS/CB. 3GPP recommends three types of cell architectures. We investigate the effects of differences between architectures upon our approach and other CoMP techniques.

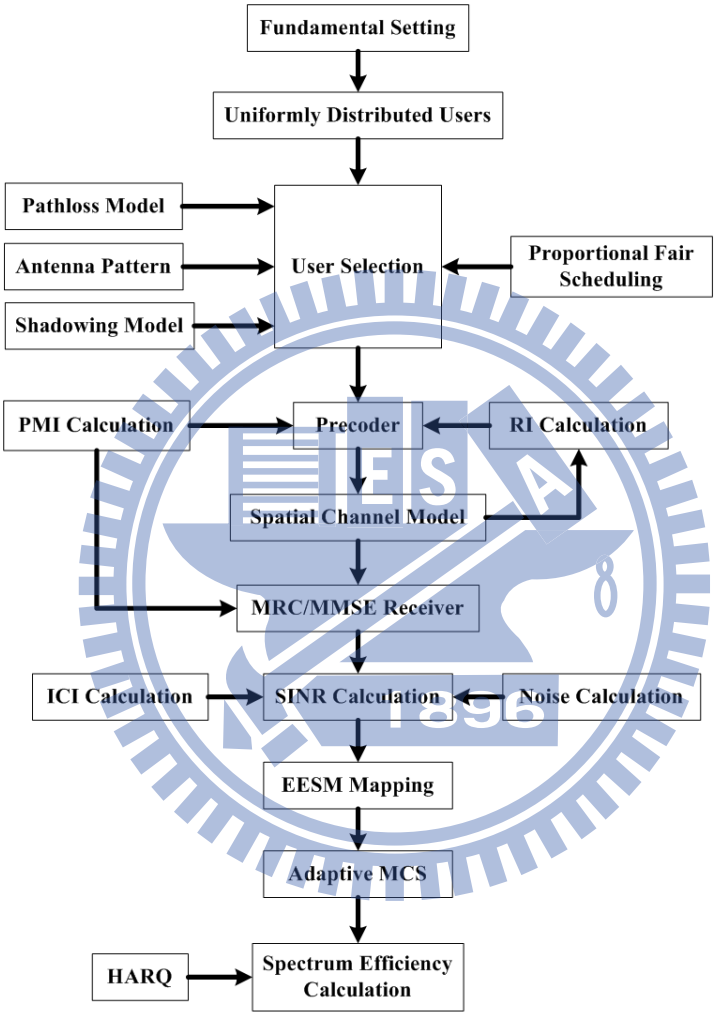

Figure 5.1: Flow chart for the physical layer simulator.

Table 5.1: **Simulation parameters for MIMO systems.**

Parameter	**Value**
Duplex Method	FDD
DL Transmission Scheme	OFDMA
Subcarrier Number	600
Downlink Transmit Antenna Number	2 and 4
Downlink Receive Antenna Number	2
ISD	500 meters
Macro-cell Number	19
Number of Users per Sector	10
User Speed	3 km/hr
Network Synchronization	synchronization
Downlink Scheduler	proportional fair scheduling in time and frequency
Downlink ARQ	a maximum of four transmission times
Downlink Receiver Type	MMSE
BS Transmit Power	46 dBm
Noise Power Density	−174 dBm/Hz
Antenna Configuration at Receiver	0.5 wavelength separation
Antenna Configuration at Transmitter	10 wavelength separation
Minimum Distance between user and macro-cell	35 meters
Channel Model	SCM urban macro
Antenna Pattern	$A_H(\phi) = -\min\left[12\left(\frac{\phi}{\phi_{3dB}}\right), A_m\right]$ $\phi_{3dB} = 70°, A_m = 25dB$
Penetration Loss	20 dB
Pathloss Model	$128.1 + 37.6\log_{10}(d)$, d in km
Shadowing Model	lognormal with zero mean and 8 dB standard deviation

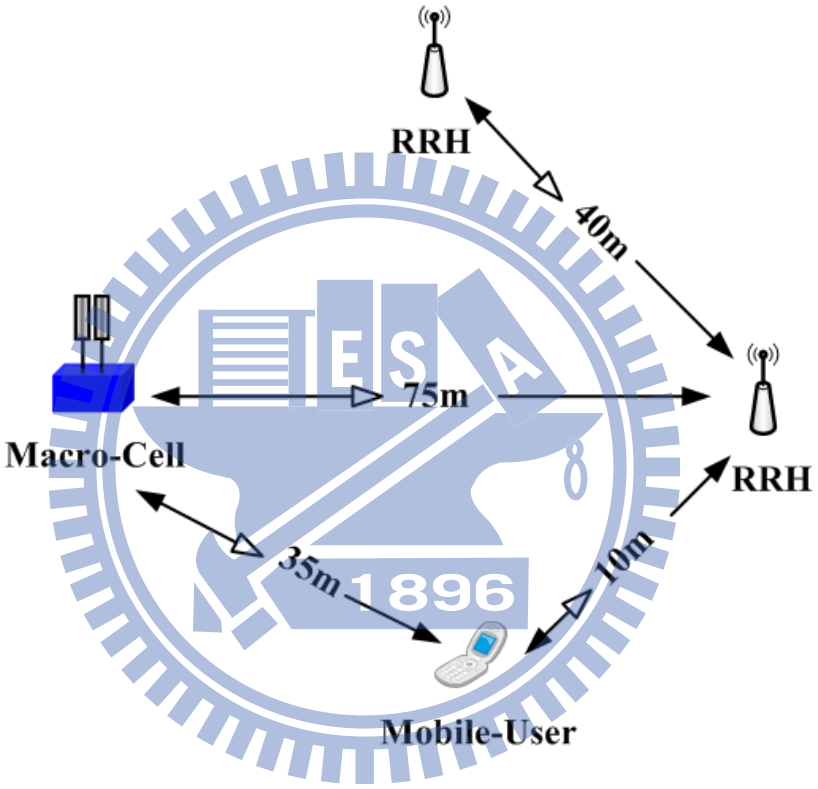

Figure 5.2: Minimum distance between devices.

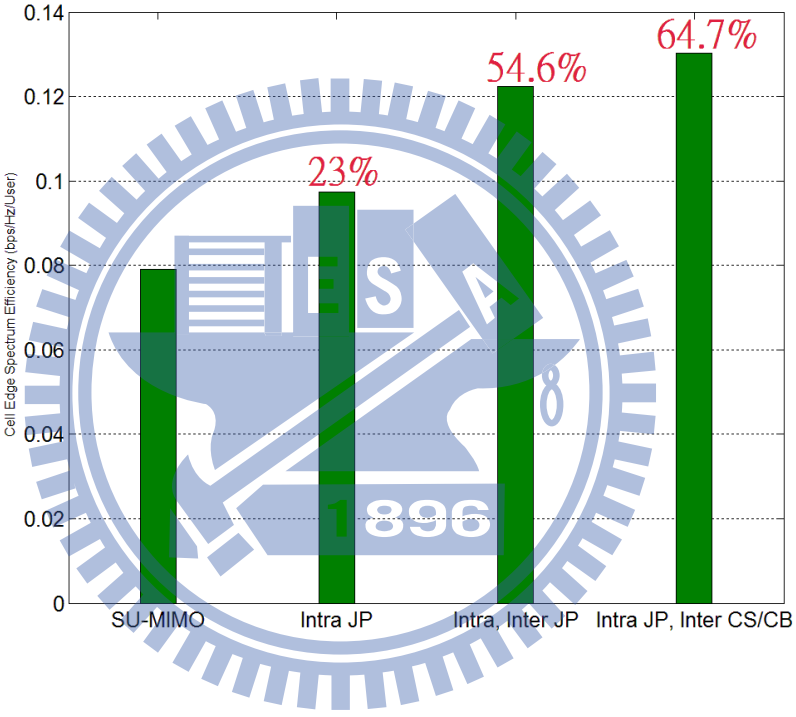

Figure 5.3: Comparisons of different CoMP schemes at the cell edge.

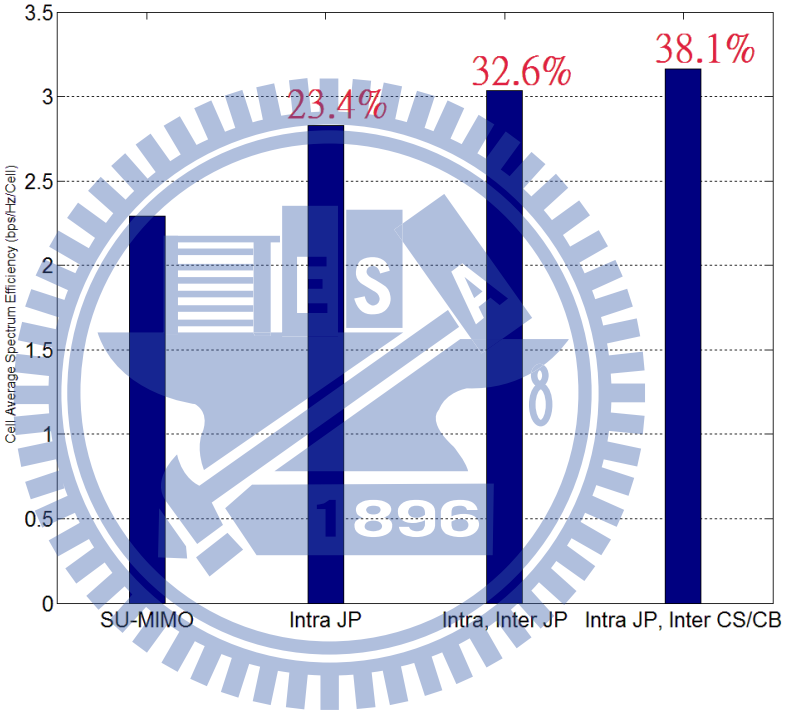

Figure 5.4: Comparisons of cell average performance for different CoMP schemes.

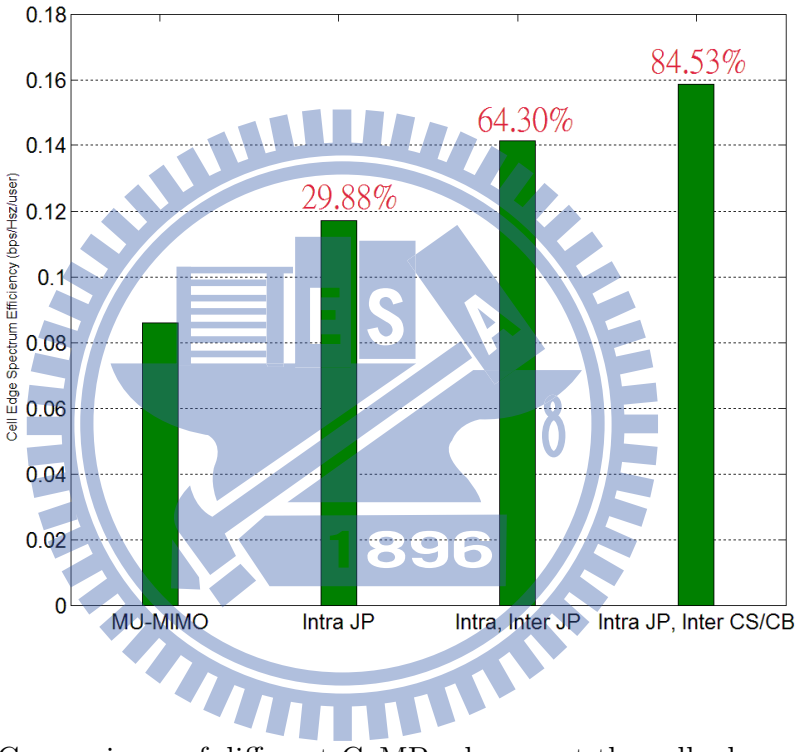

Figure 5.5: Comparisons of different CoMP schemes at the cell edge versus SU/MU-MIMO switching.

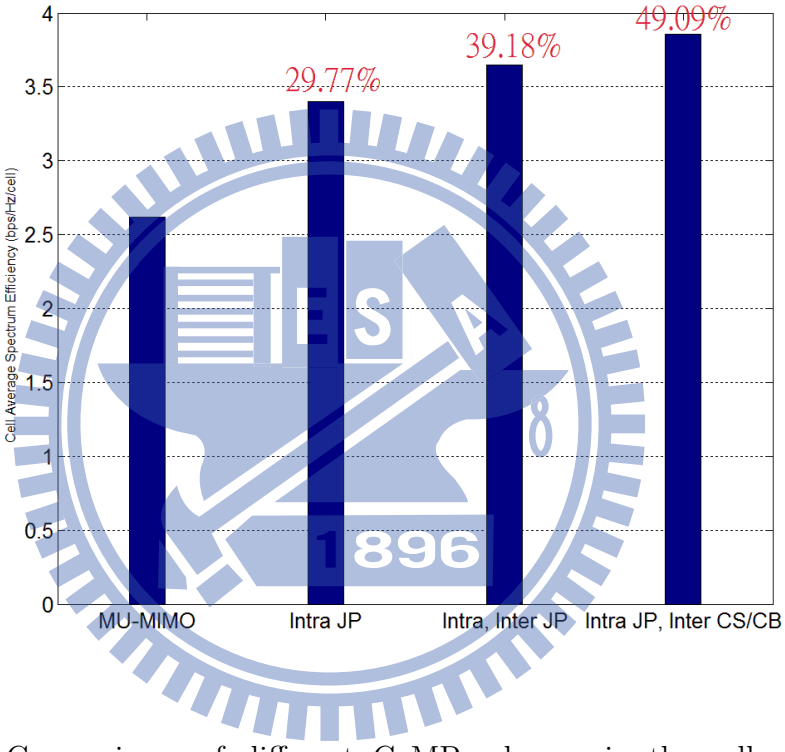

Figure 5.6: Comparisons of different CoMP schemes in the cell average versus SU/MU-MIMO switching.

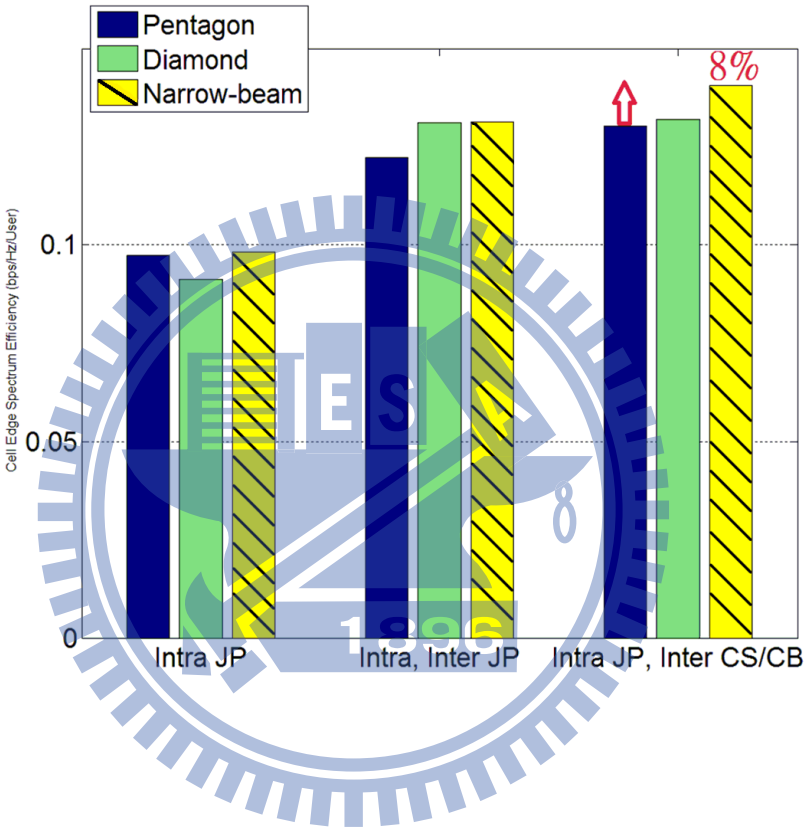

Figure 5.7: CoMP schemes performance with different cell architectures at the cell edge.

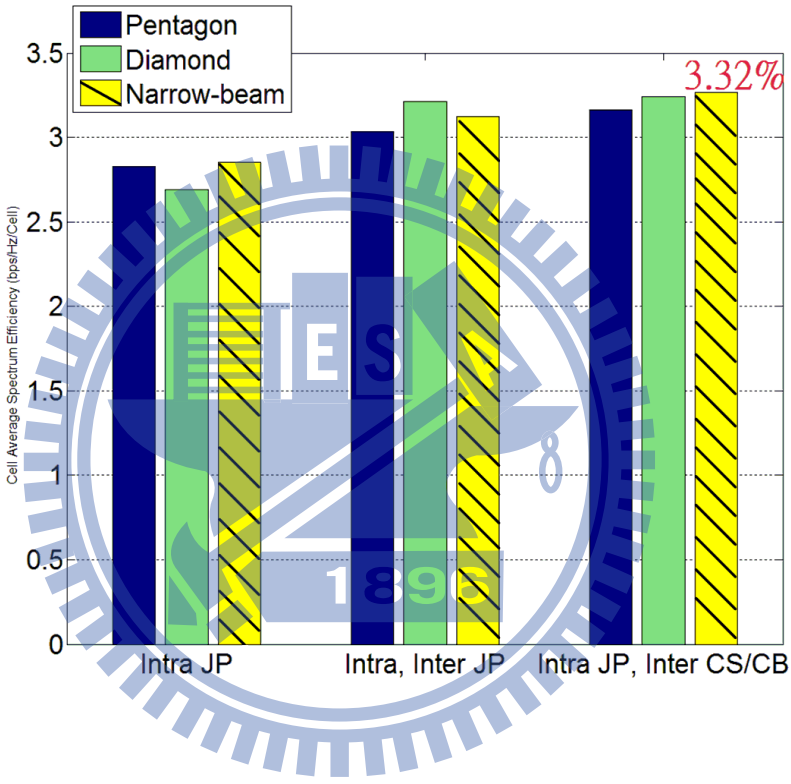

Figure 5.8: CoMP schemes performance differences for different cell architectures in the entire cell.

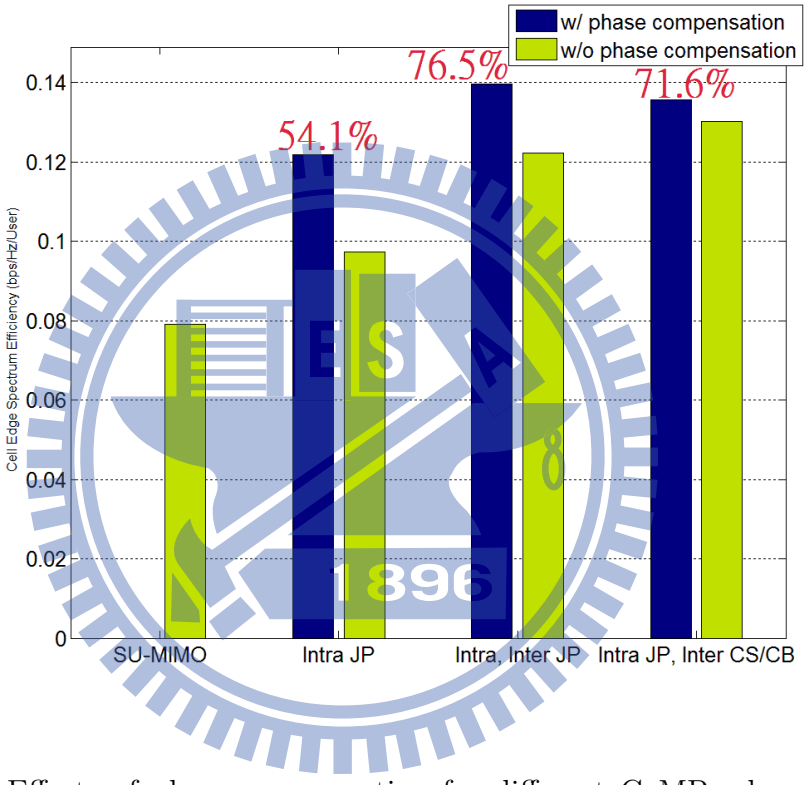

Figure 5.9: Effects of phase compensation for different CoMP schemes at the cell edge.

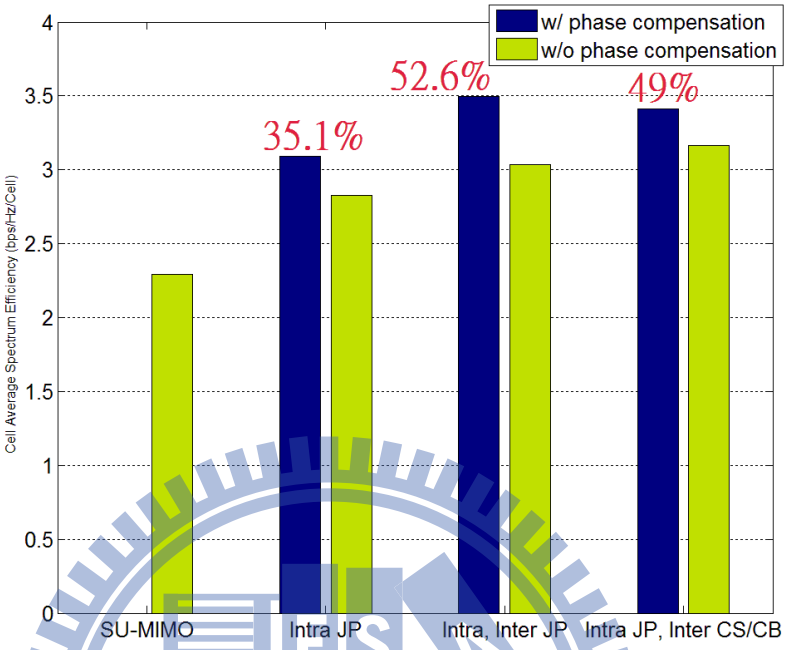

Figure 5.10: Effects of CoMP schemes performance on the cell average.

	Cell Avg.		Cell Edge	
	bps/Hz/Cell	Performance Gain	bps/Hz/User	Performance Gain
SU-MIMO	2.29	0%	0.0791	0%
Intra JP	2.8267	23.43%	0.0973	23.0%
Intra JP (phase compensation)	3.0931	35.07%	0.1219	54.11%
Intra, Inter JP	3.0366	32.60%	0.1223	54.61%
Intra, Inter JP (phase compensation)	3.4940	52.58%	0.1396	76.49%
Intra JP, Inter CS/CB	3.1618	38.07%	0.1303	64.73%
Intra JP, Inter CS/CB (phase compensation)	3.4128	49.03%	0.1357	71.55%

Figure 5.11: CoMP schemes performance gain with and without phase compensation.

CHAPTER 6

Conclusions

6.1 Summary

We operate coherent JP in heterogeneous networks based on 3GPP LTE standard [3] and obtain a better performance than non-coherent JP. However, it needs more information about channel state and leads to larger overhead. Now we consider delay effect with over two frames of delay time, which degrades performance significant. Based on the ICI mitigation beamforming design, we present a joint cooperation design of CoMP techniques in both the intra- and inter-site, and it is a feasible method to further improve the system performance. When we try to extend the cooperative range from the intra-site to inter-site, we find that the CS/CB transmission techniques in the inter-site is more effective and efficient than JP. Since this approach provides more relative gain and needs less backhaul requirement, we suggest that the joint cooperation design can be JP in intra-site and CS/CB in inter-site. The narrow-beam tri-sector architecture is the most suitable cell architecture for the inter-CS/CB plus intra-JP CoMP scheme. Our proposed scheme needs less feedback information and can further enhance the spectrum efficiency.

6.2 Future Research

The following issues are worth-while for further investigating:

1. *Feedback Design Issues:* Although we use CoMP schemes to further enhance the system performance, different schemes will need their corresponding CSI, which leads to feedback delay. Thus, it is important to discussion about which feedback components are necessary. There is a tradeoff between the amount of feedback information and the performance gain. We are supposed to suppress the feedback overhead of different CoMP schemes and control the feedback delay effect.

2. *Scheduling in Cooperation Set Issues:* Since we have proposed an inter-site CB design, we will need a master scheduler when the cooperation set is larger. A master scheduler can manage all coordinated PMI in the cooperation set and make cells use certain PMIs to make sure that the entire system throughput is maximum. This can be easily operated when three cells are coordinated. However, as the number of cooperation cells increases, deciding which users are served and which PMIs are used becomes a complicated issue.

Bibliography

[1] 3GPP, "Evolved universal terrestrial radio access (E-UTRA); further advancements for E-UTRA physical layer aspects," 3GPP, Tech. Rep. TR 36.814 V9.0.0, Mar. 2010.

[2] L. Qiang, Y. Yang, F. Shu, and W. Gang, "Coordinated beamforming in downlink CoMP transmission system," in *International ICST Conference on Communications and Networking in China (CHINACOM)*, pp. 1 –5, Aug 2010.

[3] 3GPP, "Coordinated multi-point operation for LTE physical layer aspects," 3GPP, Tech. Rep. TR 36.819 V11.0.0, Sep. 2011.

[4] 3GPP, "Design consideration for CoMP joint transmission," 3GPP, Tech. Rep. R1-091232, Mar. 2009.

[5] 3GPP, "Inter-cell interference mitigation through limited coordination," 3GPP, Tech. Rep. R1-082886, Aug. 2008.

[6] 3GPP, "CoMP with lower Tx power RRH in heterogeneous network," 3GPP, Tech. Rep. R1-110867, Feb. 2011.

[7] S. Sesia, I. Toufik, and M. Baker, *"LTE - the UMTS Long Term Evolution from Theory to Practice, second edition," Wiley*, Mar. 2011.

[8] L. C. Wang and C. J. Yeh, "A three-cell coordinated network MIMO with fractional frequency reuse and directional antennas," in *IEEE International Conference on Communications*, pp. 1–5, May 2010.

[9] R. Irmer, H. Droste, P. Marsch, M. Grieger, G. Fettweis, S. Brueck, H.-P. Mayer, L. Thiele, and V. Jungnickel, "Coordinated multipoint: concepts, performance, and field trial results," *IEEE Communications Magazine*, vol. 49, no. 2, pp. 102 –111, Feb. 2011.

[10] D. Lee, H. Seo, B. Clerckx, E. Hardouin, D. Mazzarese, S. Nagata, and K. Sayana, "Coordinated multipoint transmission and reception in LTE-advanced: deployment scenarios and operational challenges," *IEEE Communications Magazine*, vol. 50, no. 2, pp. 148 –155, Feb. 2012.

[11] Y. J. Liu, T. T. Chiang, and L. C. Wang, "Physical layer performance calibration for 3GPP LTE-A systems," in *IEEE Asia Pacific Wireless Communication Symposium*, Aug. 2011.

[12] 3GPP, "CoMP simulation assumptions," 3GPP, Tech. Rep. R1-111125, Feb. 2011.

[13] 3GPP, "Email discussion summary on calibration step 1c," 3GPP, Tech. Rep. R1-092742, Jun. 2009.

[14] 3GPP, "Physical layer aspects for evolved universal terrestrial radio access (E-UTRA)," 3GPP, Tech. Rep. TR 25.814 V7.1.0, Sep. 2006.

[15] F. Boccardi and H. Huang, "A near-optimum technique using linear precoding for the MIMO broadcast channel," in *International Conference on Acoustics, Speech and Signal Processing*, pp. III–17 –III–20, Apr. 2007.

[16] L. Thiele, T. Wirth, M. Schellmann, Y. Hadisusanto, and V. Jungnickel, "MU-MIMO with localized downlink base station cooperation and downtilted antennas," in *International Conference on Communications Workshops*, pp. 1 –5, Jun. 2009.

[17] N. Jindal, "Antenna combining for the MIMO downlink channel," *IEEE Transactions on Wireless Communications*, vol. 7, no. 10, pp. 3834 –3844, Oct. 2008.

[18] F. Shu, W. Gang, X. Yue, and L. Shao-qian, "Multi-user MIMO linear precoding with grassmannian codebook," in *International Conference on Communications and Mobile Computing*, pp. 250 –255, Jan. 2009.

[19] 3GPP, "Proposal for UE receiver assumption in CoMP simulations," 3GPP, Tech. Rep. R1-110586, Jan. 2011.

[20] J. Zhu, J. Liu, X. She, and L. Chen, "Investigation on precoding techniques in E-UTRA and proposed adaptive precoding scheme for MIMO systems," in *Asia-Pacific Conference on Communications*, pp. 1 –5, Oct. 2008.

[21] R. Heath and A. Paulraj, "Switching between diversity and multiplexing in MIMO systems," *IEEE Transactions on Communications*, vol. 53, no. 6, pp. 962 – 968, june 2005.

[22] 3GPP, "Dynamic SU/MU mode switching and rank adaptation," 3GPP, Tech. Rep. R1-092646, Jun. 2009.

[23] 3GPP, "Considerations on downlink MU-MIMO," 3GPP, Tech. Rep. R1-094278, Oct. 2009.

[24] 3GPP, "CoMP phase 1 evaluation results," 3GPP, Tech. Rep. R1-111290, May 2011.

[25] 3GPP, "Evolved universal terrestrial radio access (E-UTRA) physical layer procedures," 3GPP, Tech. Rep. TS 36.213 V9.3.0, Sep. 2010.

[26] J. C. Ikuno, M. Wrulich, and M. Rupp, "System level simulation of LTE networks," in *IEEE Vehicular Technology Conference*, pp. 1–5, May 2010.

Vita

Chen-Hsiao Chou was born in Taiwan, R. O. C. in 1988. He received his B.S. at the Department of Communications Engineering, National Chiao-Tung University in 2010. From July 2010 to August 2012, he worked his Master degree in the Mobile Communications and Cloud Computing Lab at the Institute of Communication Engineering at National Chiao-Tung University. His research interests are in the field of wireless communications.